On the combination of the planktonic foraminiferal Mg/Ca, clumped (Δ_{47}) and conventional ($\delta^{18}O$) stable isotope paleothermometers in palaeoceanographic studies

Marion Peral [1,2] (marion.peral@vub.be),
Franck Bassinot [1] (franck.bassinot@lsce.ipsl.fr),
Mathieu Daëron [1] (daeron@lsce.ipsl.fr),
Dominique Blamart [1] (dominique.blamart@lsce.ipsl.fr),
Jérôme Bonnin [3] (jerome.bonnin@u-bordeaux.fr),
Frans Jorissen [4] (frans.jorissen@univ-angers.fr),
Catherine Kissel [1] (catherine.kissel@lsce.ipsl.fr),
Elisabeth Michel [1] (elisabeth.michel@lsce.ipsl.fr),
Claire Waelbroeck [5] (claire.waelbroeck@locean.ipsl.fr),
Helene Rebaubier [1] (helene.rebaubier@lsce.ipsl.fr),
William R Gray [1] (william.gray@lsce.ipsl.fr)

(1) Laboratoire des Sciences du Climat et de l'Environnement, LSCE/IPSL, CEA-CNRS-UVSQ, Université Paris-Saclay, France
(2) Now at Analytical-Environmental and Geo-Chemistry, Vrije Universiteit Brussel, Belgium
(3) Université de Bordeaux, CNRS, Environnements et Paléoenvironnements Océaniques et Continentaux (EPOC), UMR 5805, Allée Geoffroy St Hilaire, 33615 Pessac Cedex, France
(4) UMR CNRS 6112 LPG-BIAF Bio-Indicateurs Actuels et Fossiles, Université d'Angers, 2, Boulevard Lavoisier, 49045 Angers Cedex, Franc
(5) LOCEAN/IPSL, Sorbonne Université-CNRS-IRD-MNHN, UMR7159, Paris, France

This paper is a non-peer reviewed preprint. The preprint was submitted to Geochimica et Cosmochimica Acta journal for peer review and is currently in review

Twitter: @MarionPeral

Abstract

Assuming that foraminiferal clumped isotope (Δ_{47}) values are independent of seawater salinity and pH, the combination of Mg/Ca, $\delta^{18}O$ and Δ_{47} values, may in theory allow us to disentangle the temperature, salinity/$\delta^{18}Osw$ and pH signals. Here, we present a new Mg/Ca-Δ_{47} dataset for modern planktonic foraminifera, from various oceanographic basins and covering a large range of temperatures (from 0.2 to 25.4 °C). These measurements were performed on the same samples and species as the ones used for the foraminiferal Δ_{47} calibration of Peral et al. (2018), allowing comparison between both Mg/Ca and Δ_{47} paleothermometers (excluding the two benthic foraminiferal data points). There is a good agreement between these two paleothermometers when the Mg/Ca-temperature is corrected for seawater salinity and pH, suggesting that foraminiferal Δ_{47} may not be influenced by salinity or pH. However, our results show that Δ_{47} temperature uncertainties still limit our ability to reconstruct pH and $\delta^{18}O_{sw}$ from the combination of Mg/Ca, $\delta^{18}O$ and Δ_{47} in a useful manner. We also find that disagreements between Mg/Ca and Δ_{47} values in *G. bulloides* persist after correction for vital, salinity and pH effects, suggesting that other process(es) may also influence Mg/Ca in this species.

This study also provides an updated I-CDES version of the previously published planktonic and benthic foraminiferal Δ_{47} calibration of Peral et al. (2018) , covering a range of temperature from -2 to 25.4 °C.

1. INTRODUCTION

The reconstruction of key physical and chemical ocean water parameters, like seawater temperature, salinity and pH, is critical to understand the processes driving past ocean and climate variations. However, precisely quantifying these parameters remains extremely challenging. Several proxies have been developed to reconstruct paleo-temperatures, but they all suffer from various limitations and biases. In his seminal work on isotopes, Harold Urey suggested that the extent by which ^{18}O was enriched in marine calcium carbonates relative to the water from which it is precipitated, could be used as a past ocean thermometer (Urey, 1947). However, later studies showed that this paleo-thermometer is biased by the isotopic composition of the global ocean ($\delta^{18}O_{sw}$) that does not remain constant

but reflects the waxing and waning of large continental ice sheets over glacial and interglacial cycles. This signal associated with global changes in continental ice volume strongly imprints paleo-$\delta^{18}O$ records obtained from marine carbonates (Shackleton, 1967), with additional contributions from regional modifications of evaporation/precipitation to a lesser degree. Thus, it is impossible to accurately reconstruct past ocean temperature using the carbonate $\delta^{18}O$-thermometer without an independent knowledge of seawater $\delta^{18}O_{sw}$. Furthermore, interspecies differences in the $\delta^{18}O$-temperature relationship testify to the importance of physiological processes, also called "*vital" effects* (e.g. Urey et al., 1951). In order to take into account these effects, several authors developed species-specific calibrations (e.g., Bemis et al., 1998; Mulitza et al., 2003).

More recently, several studied showed that the Mg/Ca elemental ratio of foraminiferal calcite can be used to reconstruct paleo-seawater temperatures (Rosenthal et al., 1997; Lea et al., 1999; Elderfield and Ganseen, 2000). Most foraminiferal species build their shells from magnesium-poor calcite, in which the minor amount of Mg that can be substituted to Ca is temperature dependent (Oomori et al, 1987). The paleoclimatology community had great expectations regarding the combination of foraminiferal $\delta^{18}O$ and the Mg/Ca-thermometer, which could be measured from the same material allowing theoretically to disentangle temperature and $\delta^{18}O_{sw}$ signals. However, the Mg/Ca-thermometry proved to be more complex and challenging than originally expected. First, it appeared that the partitioning coefficient between Mg in seawater and Mg in the crystal matrix is not only thermodynamically controlled by temperature, but also reflects physiological or ecological processes (Rosenthal et al., 1997; Lea et al., 1999; Elderfield and Ganseen, 2000; Lea, 2014), prompting several authors to develop species-specific, empirical Mg/Ca-temperature calibrations (Nürnberg et al., 1996; Rosenthal et al., 1997; Lea et al., 1999; Erez, 2003). From the first development of the Mg/Ca paleothermometer it was shown that foraminiferal Mg/Ca is influenced by physico-chemical variables other than temperature such as bottom-water carbonate ion concentration (Elderfield et al., 2006; Rosenthal et al., 2006), as well as surface salinity (Nürnberg et al., 1996; Lea et al., 1999; Kisakürek et al., 2008; Mathien-Blard and Bassinot; 2009, Gray et al., 2018; Gray and Evans, 2019) and pH (Lea et al., 1999; Gray et al., 2018; Gray and Evans 2019), and - on time-scales longer than ~1 Ma - the Mg/Ca ratio of seawater (Evans et al, 2016). In addition, analytical procedures must be carefully considered since cleaning protocols have an effect on the measurement of Mg/Ca within foraminiferal

shells (Barker et al 2003; Pang et al., 2020 and references therein). These secondary influences on foraminiferal Mg/Ca complicate its use as a temperature proxy.

The carbonate clumped isotope method (noted Δ_{47} hereafter) is one of the most recent paleothermometers, which has been developed over the last decade (Eiler, 2007, 2011). The Δ_{47} approach is based on the quantification of subtle statistical anomalies in the abundance of doubly substituted carbonate isotopologues ($^{13}C^{18}O^{16}O^{16}O^{2-}$) relative to the random distribution of isotopes (Eiler, 2007, 2011). A slightly higher abundance of ^{13}C-^{18}O bonds is, for thermodynamical reasons, a function of temperature (Eiler, 2011; Passey and Henkes, 2012; Stolper and Eiler, 2016) and this relationship is independent of the $\delta^{18}O$ of water in which the calcification occurs (Schauble et al., 2006). Clumped isotope methodological studies have shown no evidence of vital effects (Tripati et al., 2010; Grauel et al., 2013; Peral et al., 2018; Piasecki et al., 2019; Meinicke et al., 2020) nor salinity effects (Grauel et al., 2013; Peral et al., 2018) on foraminiferal Δ_{47}. Moreover, studies dealing with non-foraminiferal carbonates (Tripati et al., 2015; Watkins and Hunt, 2015) showed a lack of pH effect (or its negligible influence) on clumped isotope. The absence of major biases would make Δ_{47} one of the most promising paleo-thermometers. However, its use is still limited because of its low temperature sensitivity and the large sample size required to significantly reduce the analytical uncertainties. Obtaining precise and high-resolution Δ_{47} records remain a challenge.

Because of non-thermal effects on Mg/Ca from foraminifer shells, recent comparisons revealed discrepancies between Mg/Ca- and Δ_{47}-derived temperatures (Peral et al., 2020; Leutert et al., 2020; Meinecke et al., 2021). These discrepancies are not linked to any specific foraminifer species (different species were used in the three studies), nor are they associated to a given oceanic basin (samples from three different regions were studied, the Mediterranean Sea, the Southern Ocean, and the Indian Ocean) or to a time period (the studies covered from the late Pleistocene to 5 million years ago). We believe that these discrepancies can be extremely informative as they may chiefly reflect vital effects and the impact of salinity and pH on the Mg/Ca-thermometer, offering theoretically the opportunity to disentangle temperature, salinity, and pH from the combination of $\delta^{18}O$, Mg/Ca and Δ_{47} in planktonic foraminifera. Planktonic foraminiferal $\delta^{18}O$ depends on temperature and $\delta^{18}Osw$, the latter being correlated with the salinity. Carbonate $\delta^{18}O$ may be combined with Δ_{47}-derived temperature to reconstruct the $\delta^{18}Osw$ (Peral et al., 2020). As Mg/Ca is influenced by

salinity and pH, pH may be obtained by paring the Mg/Ca ratio with the reconstructed temperature from Δ_{47} and salinity estimates from sea-level or from the combination of $\delta^{18}O$-Δ_{47}, following the equations described in Gray et al. (2018 and 2019). Combining $\delta^{18}O$, Mg/Ca and Δ_{47} in foraminifera may therefore prove highly useful in palaeoceanographic studies.

The relationship between Mg/Ca and Δ_{47} in modern planktonic foraminifera has been previously studied to investigate our ability to detect the potential biases associated to Fe-Mn oxide coatings, contamination and/or dissolution of foraminiferal tests (Breitenbach et al., 2018) in order to extract the best paleo-temperature estimates from non-biased measurements. However, the sensitivity of foraminiferal Δ_{47} to salinity and pH has not been given much attention so far and still needs to be examined since a potential dependence of Δ_{47} on these chemo-physical parameters would potentially explain part of the differences observed between the Δ_{47} and the Mg/Ca paleothermometers.

For the present paper, we measured Mg/Ca on the same set of samples and foraminiferal species used in the Δ_{47} calibration of Peral et al. (2018). These data make it possible to explore the sensitivity of foraminiferal Δ_{47} to salinity and pH and evaluate the potential interest and limits of combining $\delta^{18}O$, Mg/Ca- and clumped-temperatures to disentangle temperature, salinity-$\delta^{18}Osw$, and pH effects. In the process, we took advantage of re-calibrated clumped isotope data following cutting-edge methodological developments to provide a revised version of the planktonic and benthic foraminiferal clumped isotope calibration of Peral et al. (2018), that could be used for future paleoceanographic studies.

2. MATERIALS AND METHODS

2.1. Samples

We used the same samples as those used in Peral et al. (2018), which are core-tops from twelve marine sedimentary cores from different oceanographic basins in the North Atlantic, Southern, Indian and Pacific Oceans (Fig. 1). All core-tops were chronologically constrained and are from the late Holocene (Peral et al., 2018). The location of samples, the water depths of the cores, the studied species and the ages are given in Table 1. We assume no changes in temperature, salinity, and pH over the late Holocene at our core sites and use modern

hydrological atlases to estimate these data, at the location of our sites and at the living depths of the planktonic species studied here (see paragraph 2.4.). As discussed later, the recent warming and the addition of anthropogenic CO_2 to the surface ocean likely complicate the comparison of instrumental carbonate system measurements with core-top foraminiferal samples.

The core sites cover a wide range of seawater physico-chemical conditions, with temperatures ranging from 0.2 to 25 °C (for the planktonic only) and from -2 to 25 °C (including the benthic foraminifera), and with salinity ranging from 33.7 to 36.2 and pH from 7.7 to 8.1 (both for planktonic only). The top 1 cm of each sediment core-top was collected and dried overnight at 50°C. The samples were wet sieved to collect the size fraction larger than 150 μm, and the residues were dried. To limit the potential size effects on Mg/Ca, we picked the planktonic foraminifera in narrow size ranges centered around the optimal size of each species (i.e. , the size corresponding to the maximum abundance of adult shells). The optimal sizes are divided every ~50 μm (e.g., 200-250, 250-315, 315-355, 355-400, 400-450 and 450-500 μm). Each species have their size ranges (see details in Table 2).

Nine species of planktonic foraminifera and two species of benthic foraminifera were hand-picked under a binocular. For the Mg/Ca-Δ_{47} comparison, because of the differing carbonate chemistry controls on Mg/Ca in planktonic and benthic foraminifera (Lea, 1999; Elderfield et al 2006) we exclude the two benthic samples and only provide and discuss Mg/Ca data from the planktonic foraminifera samples at the optimal size fractions. For the clumped-isotope calibration, we include the benthic foraminifera data, and a large range of size as was originally done in Peral et al. (2018).

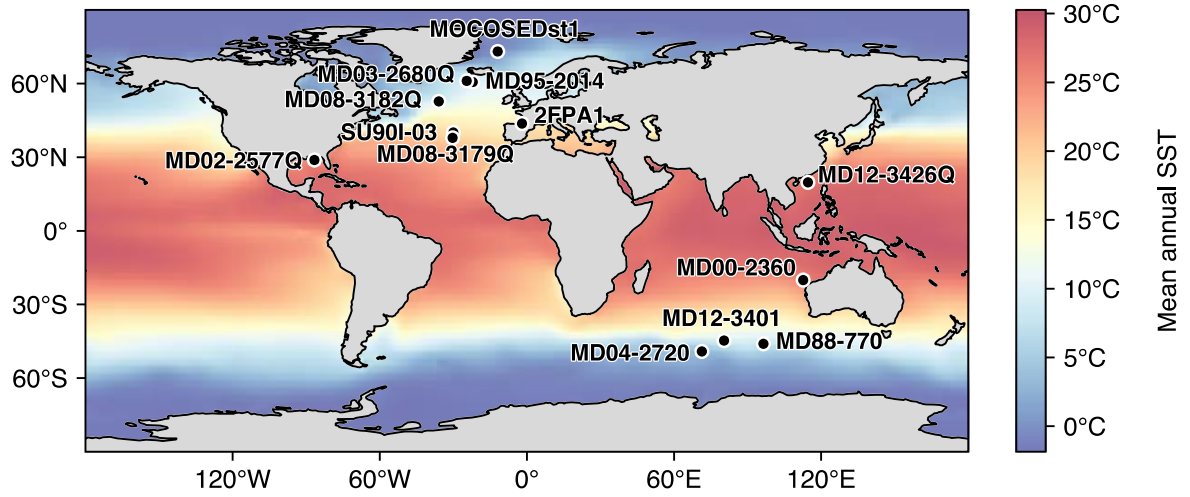

Figure 1: Map showing the location of core-tops used in this study, with the mean annual SST from WOA13

2.2. Clumped isotopes

The clumped-isotope data were previously published in Peral et al. (2018). The methodology (from the cleaning protocol to the measurement) is described in Daëron et al. (2016) and Peral et al. (2018). A summary of the cleaning protocol steps is presented in the supplementary material (Fig. S1). In the present paper, we reprocessed our Δ_{47} data in accordance with the new InterCarb - Carbon Dioxide Equilibrium Scale (I-CDES) and the associated data processing methods (Bernasconi et al., 2021; Daëron, 2021).

In previous studies, discrepancies between clumped isotope calibrations had been observed (e.g.,Tripati et al., 2010; Grauel et al., 2013). Thanks to an international effort, several laboratories conducted an intercalibration exercise in order to determine clumped isotope values of carbonate standards (ETH 1-4, IAEA-C1&2 and MERK; Bernasconi et al., 2021). This new standardization approach (I-CDES reference frame) results in internationally agreed calibrations (Anderson et al, 2021; Fiebig et al., 2021).

The Δ_{47} values of our modern foraminifera (Peral et al., 2018) were normalized to the I-CDES reference frame (Bernasconi et al., 2021) using the carbonate standards ETH-1/2/3/4. Data processing was performed using the Δ_{47}crunch library and the new pooled standardization approach, as described in Daëron (2021). The reprocessed Δ_{47} calibration is now compared with the new and/or other recalculated calibrations and used for future

paleoceanographic studies. The full dataset is provided in the supplementary material (Table S1).

The Δ_{47} values were converted to temperatures using the Peral et al. re-calculated calibration. The temperature uncertainties were estimated by propagating (i) the external Δ_{47} reproducibility of our analytical sessions of measurements, based on repeated analyses of standards and samples and (ii) the uncertainties associated with respective calibrations. Recently, Anderson et al. (2021) have shown that when using the same standardization and data processing, re-evaluated Δ_{47}-temperature calibrations obtained on various carbonate materials agree within the range of uncertainty. In terms of Δ_{47}-temperature reconstructions, using Peral et al. (2018) re-calculated calibration (this paper), or using the unified calibration from Anderson et al. (2021), yield the same results. We found it important to provide in the present paper a revised calibration equation that is based on cutting-edge approaches of Δ_{47} standardization and processing methods (Bernasconi et al. 2021; Daëron, 2021) to serve for future studies based on the state-of-the-art standard values.

2.3. Mg/Ca analyses and derived temperatures

2.3.1. Mg/Ca measurements

A total of 93 Mg/Ca analyses on 9 species of planktonic foraminifera were performed at the Laboratoire des Sciences du Climat et de l'Environnement (LSCE) using a PlasmaQuant ELITE Inductively coupled plasma mass spectrometry (ICP-MS) from Analytik Jena. One milligram of foraminiferal shells was hand-picked for each sample allowing to perform 3 to 4 replicate analyses. We followed the cleaning protocol of Barker et al. (2003). Shells were crushed between two glass plates and the resulting fragments were put into acid-leached micro-vials. Fine material (i.e. clay) was removed through repeated ultrasonic cleaning with 18.2 MΩ water and then ethanol. In order to remove potential organic contaminants, the samples were then oxidized with alkali-buffered 1% H_2O_2 solution for 10 minutes at 100°C. The final cleaning treatment consists in a rapid leaching with 0.001 M HNO_3, before dissolution in 0.15 M HNO_3. Samples are centrifuged immediately after dissolution and transferred to a new acid-leached centrifuge tube, leaving a residual ~ 10 µl, which helps exclude any

remaining undissolved contaminants. Trace metal grade (NORMATOM) acids are used throughout.

A 10 µl aliquot of each sample was first analyzed in order to determine calcium concentrations. The samples were then diluted to a calcium concentration of 1mM Ca, to match that of the bracketing standards. Mg/Ca ratios were measured using a modified version of the method of Yu et al. (2005) against in-house standards prepared from single elementary solutions. Mg/Ca instrumental precision was determined based on multiple replicates of a standard solution of known Mg/Ca composition, with a long-term precision of 2% (2RSD). Analysis of external standard NIST RM 8301 (Foraminifera) using our method gives a value of 2.65 ± 0.02 (1SE), in excellent agreement with its published value of 2.62 ± 0.14 (Stewart et al., 2020). The data are summarized in Table 2 and the full data set is provided in supplementary material (Table S2).

2.3.2. Correction of Mg/Ca for the effects of salinity and pH

We corrected our Mg/Ca values for pH and salinity effects based on the following procedure: 1) using species-dependent calibrations, we calculated at each core location the Mg/Ca values which are expected given the atlases-derived pH and salinity, and the $\delta^{18}O$-derived temperature, 2) at all the sites, we also calculated a pH- and salinity- normalized Mg/Ca values (Mg/Ca normalized) by setting pH=8 and salinity=35, and using the sample-specific oxygen isotopic-derived temperature; 3) the difference between the expected and normalized Mg/Ca values provide correction values at each site and for each species, (4) these correction values are then substracted from our measured Mg/Ca values to cancel out the salinity and pH effects from our data, thus leaving only temperature as a control parameter.

Practically, for the first step of this procedure, we used the species-specific equations (Table 3) from Gray and Evans (2019) for *Globigerinoides ruber* and *Globigerina bulloides* to estimate the "expected" Mg/Ca values. For the species for which a specific calibration is not available, we used the generic equation of Gray and Evans (2019). To the best of our knowledge, *N. pachyderma* is not pH sensitive (Tierney et al., 2019). Thus, no pH correction was applied to the Mg/Ca of this species, and it is corrected for salinity only.

The multi-parameter regression equations of Gray and Evans (2019) provide Mg/Ca as a function of the temperature, the salinity, and the pH of the sea water in which the foraminifera have grown:

$$Mg/Ca = \exp (a \times (S - a) + c \times T + d \times (pH - e) + f$$

Where a, b, c, d, e and f are constants, and T, S and pH are the temperature (in °C), the salinity and the pH of seawater during calcification. As said above, for each site and each species, we solved the regression equations using modern, atlas-derived pH and salinities, and the foraminifer $\delta^{18}O$-derived temperature (see details in section 2.4), and then proceed to steps 2 to 4 (see above).

2.3.3. Mg/Ca-derived temperatures

2.3.3.1 Multi-species calibration equation from Anand et al. (2003)

In order to compare Mg/Ca and clumped-isotope-derived temperatures, we first calculated the Mg/Ca-derived temperatures using the multi-species calibration of Anand et al. (2003) solved using our pH- and salinity- corrected Mg/Ca values. The estimated-Mg/Ca temperatures show a large difference when compared with the clumped-isotope-derived temperatures (see supplementary material, Fig. S2). We recalculated the multi-species Anand et al. (2003) calibration using the temperatures from the oxygen isotopic calibration of Kim and O'Neil (1997). This equation may provide a more robust basis for reconstructing temperature effects (Roche et al., 2018) than the modified, benthic-derived equation of Shackleton (1974) originally used in the Anand et al. (2003) study (see details in section 2.4.1). Following the same strategy as Anand et al. (2003), we only included the data from the 350 – 500 μm size-range and excluded the data from *Orbulina universa* and *Globigerinella*. We note that, as shown in Anand et al. (2003), the measured $\delta^{18}O$calcite is up to ~1 per mil too light in the wintertime compared to the value predicted using the measured sea surface temperature- and salinity-based $\delta^{18}O_{sw}$ estimates at the Sargasso Sea sediment trap site. This is likely due to a seasonal change in the $\delta^{18}O_{sw}$-salinity relationship at this site, which potentially introduces a substantial bias to the resulting Mg/Ca equation (Gray et al, 2018). The recalculated equation is presented in Table 3 and shown in supplementary material (Data Processing file).

303

304 2.3.3.2 Mono species-specific equations

305

306 We first used calibration equations that were derived by linking Mg/Ca to temperature
307 only. To the best of our knowledge, we chose the most adequate calibrations, considering the
308 species, the size fraction, the oceanic region, and the cleaning protocol. For seven of the
309 planktonic species studied in the present manuscript, we used the mono-specific equations of
310 Anand et al. (2003). Unfortunately, the only available calibration for *Globorotalia menardii*
311 was established using a cleaning protocol with a reductive step (Regenberg et al., 2010), which
312 is known to lower the Mg/Ca ratio of foraminifera compared to the cleaning approach of
313 Barker et al. (2003) that we used for the present paper (e.g., Pang et al., 2020). In the absence
314 of a calibration for *Neogloboquadrina pachyderma* (dextral), we used the same calibration as
315 the one developed for *N. pachyderma* (sinistral) (Vázquez Riveiros et al., 2016). The
316 uncertainties were calculated by propagating the analytical errors, based on the long-term
317 standard deviation of our standards and the uncertainties associated with the respective
318 calibrations.
319 It is important to underline that, for internal consistency, the mono-species calibrations were
320 corrected for local pH and salinity effects, as described in section 2.3.2. (i.e. species-specific
321 equation of Gray and Evans (2019) with isotopic temperature, and salinity and pH from the
322 atlases). For the Anand et al. (2003) calibrations, we used the *in situ* salinities available in
323 Deuser and Ross (1989). The calibration of Regenberg et al. (2010) based on *G. menardii* was
324 not corrected because we could not find the raw Mg/Ca data.

325

326 **2.4. Independent constraints on temperatures, salinity and pH from Δ_{47} and Mg/Ca ratios**

327

328 **2.4.1.** Estimation of calcification temperatures

329

330 In order to limit uncertainties associated to the imperfect knowledge of planktonic
331 foraminifera ecology, numerous authors have used $\delta^{18}O$-derived temperatures instead of
332 atlas temperatures for the calibration of geochemical proxies (e.g. Anand et al., 2003;
333 Mathien-Blard and Bassinot, 2009; Peral et al., 2018; Meinicke et al., 2020). Comparing
334 WOA13 atlas temperatures and foraminifer $\delta^{18}O$-derived temperatures obtained using

various calibration equations, Peral et al. (2018) suggested the use of the calibration equation of Kim and O'Neil (1997), modified for consistency by using an acid fractionation factor (difference of oxygen isotope ratio between the mineral (calcite) and the CO_2 gas evolved from acidification with phosphoric acid) of 1.01025 (Eq. 1). The Kim and O'Neil (1997) calibration is then used to calculate the $\delta^{18}O$-derived temperatures in this study:

$$1000 \ln(\alpha_{CC/W}) = 18.03 \times 1000 / T - 32.17 \quad \text{(Eq. 1)}$$

Where T is the isotopic temperature in Kelvin and $\alpha_{CC/W}$ is the oxygen-18 fractionation factor between calcite and water, with:

$$\alpha_{CC/W} = (1 + \delta^{18}O_{C/SMOW} / 1000) / (1 + \delta^{18}O_{SW/SMOW} / 1000) \quad \text{(Eq. 2)}$$

Where $\delta^{18}O_{C/SMOW}$ and $\delta^{18}O_{SW/SMOW}$ correspond to foraminiferal calcite and seawater $\delta^{18}O$ relative to VSMOW. Following the recommendation of Marchitto et al. (2014), $\delta^{18}O_C$ values for *Uvigerina* were adjusted by subtracting 0.47 ‰.

Seawater $\delta^{18}O$ values at each core site were extracted from the gridded data set of LeGrande and Schmidt (2006). The same approach as the WOA-temperature extraction is followed (as described in Peral et al., 2018). Because one still does not know well the exact habitat depth and growth season of planktonic species and their spatial variability in relation to nutrient availability and physico-chemical conditions (i.e., Retailleau et al., 2011; Schiebel and Hemleben, 2017), we followed the same approach as Peral et al. (2018). We calculated the $\delta^{18}O_{SW}$ of seawater in which foraminifera calcified by averaging at each site the gridded $\delta^{18}O_{SW}$ of LeGrande and Schmidt (2006) over species-specific living depth ranges. These depth ranges may vary across ocean basins. According to Tolderlund and Be´ (1971) and Durazzi (1981), living depths in the North Atlantic Ocean range between 0 – 50 m for *G. ruber* and *O. universa,* and the depth range is 0-100m for *G. bulloides, G. truncatulinoides*, *G. menardii and G. inflata* (Steinke et al., 2005; Numberger et al., 2009, Rebotim et al 2017). For *N. pachyderma*, the living depth is estimated from 0 to 200 m depth (Rebotim et al., 2017). In the Indian Ocean, Duplessy et al. (1981) placed the depth of calcification for all these species within and below the mixed layer, except for *G. ruber* and *G. menardii* which are believed to

remain respectively at the surface and within the mixed layer (0–100 m). In the South China Sea, *G. ruber* and *G. menardii* are described as living near the surface and in the top 100 m, respectively (Pflaumann and Jian, 1999). Finally, the living depth of *O. universa* being very poorly constrained to the best of our knowledge, we assume that it lives everywhere at the same depth as in the North Atlantic Ocean (Rebotim et al., 2017). For benthic foraminifera (re-calibration of clumped isotope versus temperature), we must use the bottom $\delta^{18}O_{SW}$ values. For the planktonic foraminifera, the mean $\delta^{18}O_{SW}$ values averaged for the living depth of each species for each oceanic basin is considered. The uncertainty of $\delta^{18}O_{SW}$ at each site was estimated as the quadratic sum of the site-specific standard deviation of $\delta^{18}O_{SW}$ within the corresponding water depth and a constant error of 0.20 ‰ assigned to the GISS grid interpolation. Final uncertainties of the oxygen isotopic temperatures are propagated based on the $\delta^{18}O_{SW}$ uncertainties and the external analytical error on $\delta^{18}O$ values.

For *G. bulloides* and *O. universa,* we could also compare the reconstructed Mg/Ca-temperatures to $\delta^{18}O$-temperatures obtained using the species-specific $\delta^{18}O$ calibrations from Bemis et al. (1998). This comparison is presented in Figure S3 and discussed in paragraph 4.2.

2.4.2. Estimation of seawater salinity and pH

The seawater salinity values at each core-top location were extracted from the WOA13 gridded data set (Zweng et al., 2013). As for the GISS $\delta^{18}O_{SW}$ values (see above), for each ocean basin, we computed the seawater salinity in which the foraminifera calcified by averaging the atlas salinities over the living depth range known for each species. Uncertainties were estimated at each site as the quadratic sum of a nominal error of 0.20 arbitrarily assigned to the WOA13 data set and the site-specific standard deviation of salinity.

The seawater pH values at each core-top location and for each species living depth were extracted from the GLODAP 2020 data set (Olsen et al., 2020). Similarly, following the same strategy as for the GISS $\delta^{18}O_{SW}$ and WOA13 salinity, we averaged the available GLODAP 2020 data over the living depth-range published for each species. A pH uncertainty of 0.02 was assigned to GLODAP pH data (Olsen et al., 2020). We note that this only represents a 'climatological' error. The use of climatological pH data is far from ideal because, due to the release of anthropogenic CO_2, the surface ocean has acidified considerably since 1850. This

has lowered the pH relative to the pre-industrial value, whereas the vast majority of foraminifera retrieved in the core top samples are likely to be of preindustrial age or older. This pH uncertainty represents a major source of uncertainty in our analysis and is a major hindrance to usefully constraining the sensitivity of foraminiferal proxies to the carbonate system using coretop material.

3. RESULTS

3.1. Clumped isotope dataset

The clumped-isotope calibration using the same data set as Peral et al. (2018) is recalculated following the latest methodological developments (see section 2.2 for details). The recalculated clumped-isotope data range from 0.6976 ‰ to 0.5917 ‰ and cover a range of temperatures from -2.3 to 25.4 °C (oxygen isotopic temperatures from eq. 1 are used in the whole section; Table 2). As expected, the Δ_{47} values increase with decreasing temperatures; the benthic foraminifera sample from the artic (*C. wuellerstorfi* – MOCOSED-St1) shows the highest Δ_{47} value, while planktonic foraminifer sample from one of the warmest sites *G. ruber* – MD00-2360) shows the lowest Δ_{47} value.

3.2. Raw Mg/Ca dataset

We only measured Mg/Ca for the planktonic foraminifera. Our raw Mg/Ca dataset ranges from 0.8 to 7.7 mmol/mol (Table 2 for the whole section) and covers a range of temperatures from -0.7 to 25.4 °C (temperatures for the whole section; Table 2). As expected, the cold-water dwelling foraminifera (*N. pachyderma* s. – MOCOSED st 1) show the lowest Mg/Ca values and the warm-water surface dwellers such as *G. ruber* and *O. universa* show the highest Mg/Ca values. Note the particularly high value (Mg/Ca =7.7 mmol/mol) obtained for O. universa . This species likely calcifies at a lower temperature than *G. ruber*, which nevertheless shows a raw Mg/Ca value of only 4.3 mmol/mol (sample of MD00-2360). Our data therefore support previous observations that *O. universa* is characterized by unusually high Mg/Ca ratios (Lea, 1999; Anand et al., 2003).

The raw Mg/Ca ratios measured on the same samples and species, but for different size fractions, show a maximum difference of 0.4 mmol/mol between all the size fractions.

3.3. Corrected Mg/Ca

The raw Mg/Ca values are corrected for salinity and pH from atlas data, using the method as described in section 2.3.2. The corrected Mg/Ca, excluding *N. pachyderma* samples, ranges from 1.6 mmol/mol (Table 2) for *G. bulloides*-MD12-3401 that calcified at 5 °C (isotopic temperatures, Table 2), to 4.9 for *G. ruber*-MD00-2360 that calcified at 24.8 °C (isotopic temperatures, Table 2). It is also noticeable that *G. bulloides* species still records high Mg/Ca values, as discussed in part 4.3. For a better comparison between our Δ_{47} and Mg/Ca values, we test all subsequent analysis with and without G. bulloides in the dataset. The corrected Mg/Ca values for the species coming from the same core tops display a consistent relationship with calcification temperatures.

3.4. Comparison of Mg/Ca-derived temperatures (multi-species and mono-species equations) with $\delta^{18}O$ and Δ_{47}-derived temperatures

The Mg/Ca-derived temperatures were estimated using the recalculated multi-species calibration of Anand et al. (2003) and compared to the $\delta^{18}O$-temperatures (Fig. 2.a) estimated using Kim and O'Neil (1997) equation (eq. 1), as described in section 2.4.1. The Mg/Ca-temperatures for the species *G. bulloides* are systematically higher than the $\delta^{18}O$-derived temperatures, while most of the other species display lower Mg/Ca-derived temperatures (Fig. 2.a). A linear regression only explains 57 % of co-variance between the two thermometers (Fig. 2.a).

Then, the Mg/Ca-derived temperatures reconstructed using the multi-species calibration of Anand et al. (2003) are compared to the Δ_{47}-derived temperatures obtained using the recalculated version of the foraminifer calibration equation of Peral et al. (2018; see section 2.3; Fig. 2.b). As was observed with the $\delta^{18}O$-temperatures, the *G. bulloides* species show higher Mg/Ca-derived temperatures than those derived from Δ_{47} and a linear regression only explains 52 % of co-variance between the two thermometers (Fig. 2.b).

We then computed Mg/Ca-derived temperatures using mono-species calibrations. These Mg/Ca-temperatures are in better agreement with $\delta^{18}O$-derived temperatures (Table 3; Fig. 2.c) and Δ_{47}-derived temperatures (Fig. 2.d.), with regression equations explaining 80 % and 76 % of co-variance. However, Mg/Ca-derived temperatures are always warmer than the isotopic temperatures.

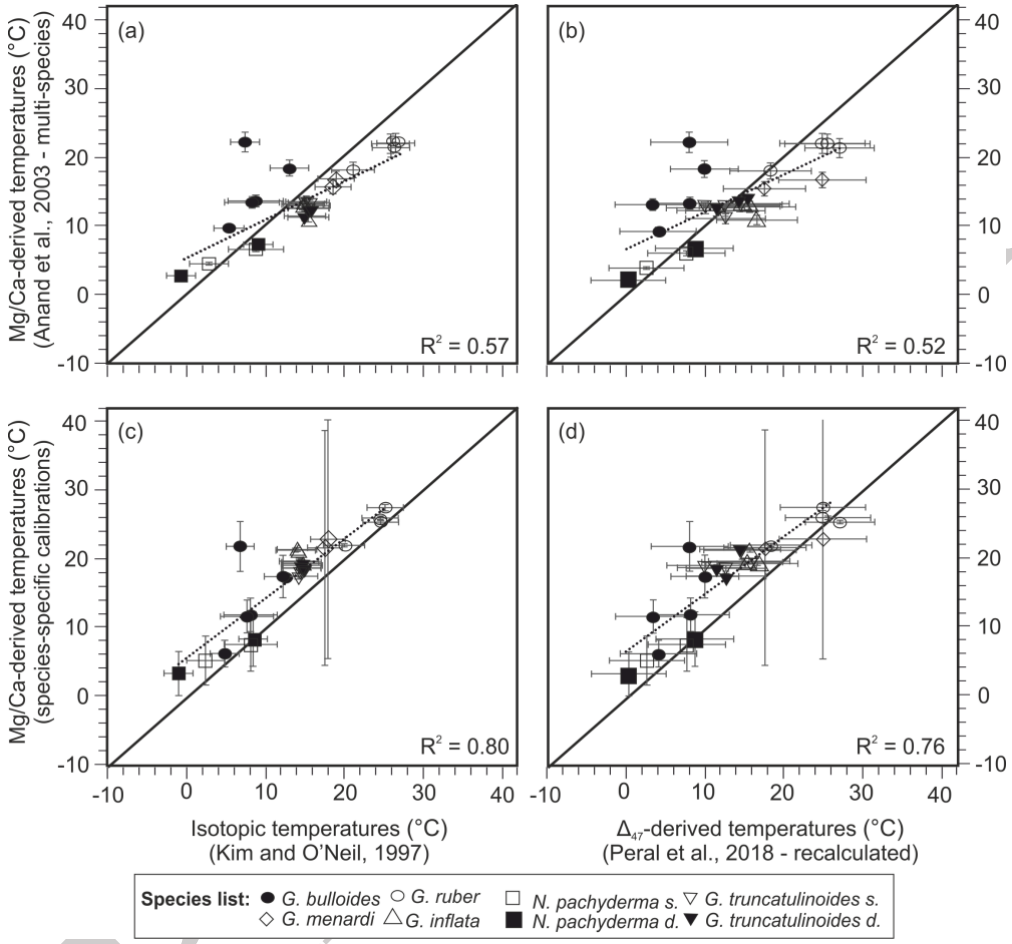

Figure 2: Comparison of temperature estimates obtained on 9 planktonic species. Top panels: reconstructed Mg/Ca temperatures using the recalculated multi-species calibration of Anand et al. (2003) compared to reconstructed $\delta^{18}O$ temperatures, using Kim and O'Neil (1997) (a) and Δ_{47}-derived temperatures, using the recalculated calibration equation of Peral et al. (2018) (this paper) (b). Bottom panel: reconstructed Mg/Ca derived temperatures using the most adequate mono-specific calibrations compared to reconstructed $\delta^{18}O$ temperatures, using Kim and O'Neil (1997) (c) and Δ_{47}-derived temperatures, using recalculated Peral et al. (2018) calibration (d). Dotted black lines are linear regressions, the black solid lines are the 1:1 line. Uncertainties are at 2SE.

3.5. Δ_{47} values versus raw, corrected Mg/Ca values

The Δ_{47} values (recalculated from the raw data of Peral et al., 2018) are compared to (1) the raw Mg/Ca values (Fig. 3.a – without *O. universa*), (2) the Mg/Ca values corrected for seawater salinity only (i.e. setting d constant to zero in the correction equations from Gray and Evans, 2019) (Fig. 3.b), and (3) the Mg/Ca values corrected for both seawater salinity and pH salinity (Fig. 3.c).

The raw Mg/Ca data (without corrections) show a poor agreement with the Δ_{47} values (Fig. 3.a; $R^2 = 0.52$). Similarly, poor agreement is observed using either "salinity" corrected Mg/Ca or "salinity + pH" corrected Mg/Ca. ” ($R^2 = 0.51$ in Fig. 3.b & c). However, it should be noted that without the *G. bulloides* samples, the agreements for the three comparisons improve significantly with an R^2 of 0.90, 0.90 and 0.89, respectively (Fig. 3.a&b&c).

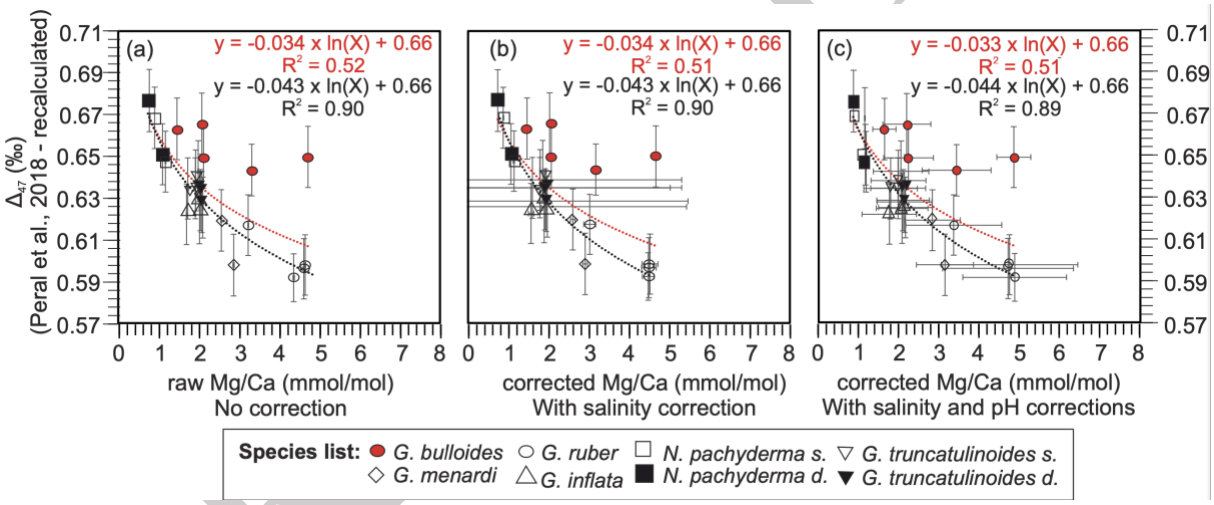

Figure 3: Comparison of our recalculated foraminiferal Δ_{47} values with raw Mg/Ca values (uncorrected) (a), with corrected Mg/Ca for salinity only (b), and with corrected Mg/Ca for salinity and pH (c). The Mg/Ca values are corrected using the equations from Gray and Evans (2019), the salinity and pH from the atlas and the oxygen isotopic temperatures. The red dotted logarithmic regressions are plotted for all the plots, including *G. bulloides* and the black regressions are without *G. bulloides*. All the uncertainties are at 2SE.

4. DISCUSSION

4.1. Updated foraminiferal clumped-isotope calibration

The efforts of the clumped-isotope community have led to the establishment of an international standardization and a uniform measurement data processing, allowing robust/accurate comparisons between Δ_{47} measurements performed in different laboratories (Bernasconi et al., 2021, and Fig. 4 therein). Following the newest methodological advancements in clumped isotope – new standard values and data processing (see details in section 3.2) - (Bernasconi et al., 2021; Daëron, 2021), we recomputed the multi-foraminiferal species calibration from Peral et al. (2018) (Fig. 4). The total least squares regression yields the following relationship:

$$\Delta_{47} = A \times 10^3 / T^2 + B \qquad \text{eq. 3}$$

Where A = 37.0 and B = 0.181

To compute the formal standard errors for this regression, we reformulate the equation 3 in terms of the barycenter of our ($1/T^2_0$) values, so that parameters A and B0 are statistically independent:

$$\Delta_{47} = A*(T^{-2} - T_0^{-2}) + B_0 \qquad \text{eq. 4}$$

Where A = 37.0 (SE = 2.0), B_0 = 0.636 (SE = 0.0025) and T_0 = 285.1 K

The conclusions drawn by Peral et al. 2018) based on the original data, are still valid – i.e. no apparent species-specific foraminiferal size and salinity effects (cf. Peral et al., 2018 for more details). The updated calibration established in the present paper is compared with the unified calibration of Anderson et al. (2021) and the precise inorganic calibration of Fiebig et al. (2021) (Fig. 4). A good agreement (in the range of 0.3 – 1.3 °C, within the calibration uncertainties) is observed between the three calibrations. This agreement between biogenic carbonates (this study) and inorganic carbonates (Anderson et al., 2021; Fiebig et al., 2021 and the slow-growing Laghetto Basso and Devils Hole calcite (Daeron et al., 2019; Anderson et al., 2021)) confirms that using standardized protocols (Bernasconi et al., 2021; Daëron, 2021) solves the large discrepancy between the calibrations (Anderson et al., 2021; Fiebig et al., 2021). Also, this calibration constitutes the more precise equation based on foraminifera.

These observations allow a direct application of this calibration to foraminifera for palaeoceanographic studies; this recalculated version of the calibration by Peral et al. (2018) should be used instead of the original version for future paleoceanographic studies.

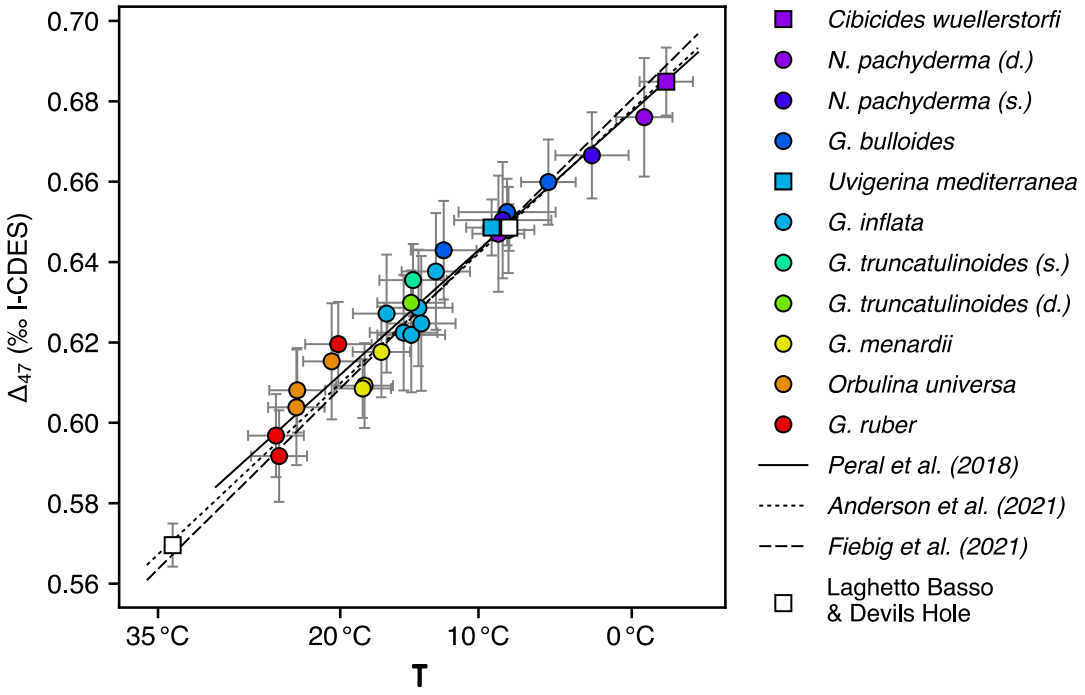

Figure 4: Recalculated Δ_{47} values (mean and 2SE) compared to oxygen isotopic temperatures (mean and 2SE) obtained with Kim and O'Neil (1997) for planktonic (circle) and benthic (square) foraminifera samples, combining all size fractions (modified from Peral et al., 2018). The new calibration regression corresponds to the black line (Peral et al., 2018 recalculated). The recalculated foraminiferal calibration is compared to the slow-growing calcite from Laghetto Basso and Devils Hole (from Anderson et al., 2021) and to calibrations of Anderson et al. (2021) and Fiebig et al. (2021)

4.2. Species specific effects on Mg/Ca-temperatures vs Δ_{47}-temperatures comparison

By comparing various paleothermometers we are able to better constrain the limitations of each of the methods and, within the framework of these limitations, try to extract as much meaningful climatic information as possible by combining those proxies.

The plot of Mg/Ca-temperatures vs Δ_{47}-derived temperatures (Fig. 2.b) shows a larger scattering around the 1:1 line than the plot displaying Mg/Ca-temperatures vs δ^{18}O-derived

temperatures (Fig. 2.a). This larger scattering likely results from the higher uncertainties in the clumped-isotope-derived temperatures. The use of species-specific calibrations for Mg/Ca-derived temperatures improves the fit with the Δ_{47}-derived temperatures, compared to the use of a multi-species calibration (Fig. 2.d vs Fig. 2.b). No species-specific calibration is necessary for clumped isotope as Δ_{47} thermometer does not appear to be affected by species-specific effects (Tripati et al., 2010; Grauel et al., 2013; Peral et al., 2018; Meinicke et al., 2020).

Although R^2 values significantly increase when using species-specific Mg/Ca calibrations, the Mg/Ca-derived temperatures are systematically warmer than $\delta^{18}O$- and Δ_{47}-derived temperatures (Fig. 2.b&d – linear regression lines). This is coherent with previous observations (Peral et al., 2020; Leutert et al., 2020).

No significant improvement is observed when species-specific calibrations are used to reconstruct temperatures from *G. bulloides* and *O. universa* $\delta^{18}O$ (Bemis et al., 1998) (Figure S3). *G. bulloides* Mg/Ca data result in temperatures as high as 20 °C, showing up to 12 °C difference with the two isotopic thermometers (see discussion below in section 4.3.). One second explanation would be the dependance of Mg/Ca values on salinity and pH (Nürnberg et al., 1996; Kisakürek et al., 2008; Mathien-Blard and Bassinot, 2009, Gray et al., 2018; Gray and Evans, 2019). It has been shown that the Δ_{47} in foraminifera is not affected by salinity (Tripati et al., 2010; Peral et al., 2018), however, the pH dependence of the foraminiferal Δ_{47} thermometer has never been studied to this date. By comparing both foraminiferal-Δ_{47} and corrected-Mg/Ca temperatures, the potential effect of pH on clumped isotopes can be deciphered.

4.3. *G. bulloides* species in Mg/Ca

The relatively poor correlation between raw or corrected Mg/Ca and clumped isotope (Fig. 3a&b&c) chiefly results from particularly high *G. bulloides* Mg/Ca values and the high variability of *G. bulloides* data over a narrow Δ_{47} range (Fig. 3a&b&c). The correlations significantly improve when *G. bulloides* samples are excluded. The high Mg/Ca ratios measured in *G. bulloides* and their important variability are not explained by anomalous, local salinity or pH values. High *G. bulloides* Mg/Ca values could be likely explained by 1) diagenesis or metal coating, 2) pH effect on $\delta^{18}O$ measurements or 3) the existence of different *G.*

bulloides morphotypes and/or genotypes characterize by different temperature-driven Mg/Ca incorporation mechanisms.

1) Diagenesis or metal coating: The relationship between foraminiferal Δ_{47} and raw Mg/Ca has been previously examined by Breitenbach et al. (2018). These authors suggested that the clumped isotope-Mg/Ca comparison could help identify potential problems and biases of the Mg/Ca-thermometer resulting from Fe-Mn oxide coatings, clay contamination and/or foraminiferal test dissolution. Our foraminifera samples are in a good state of preservation and do not suffer from dissolution (SEM pictures available in Peral et al., 2018). Additionally, the Fe/Ca and Mn/Ca values are low in our dataset, below the thresholds that lead to suspect a contamination problem (Boyle and Keigwin (1985); see supplementary material Table S2). Nevertheless, the *G. bulloides* sample showing the highest Mg/Ca value (sample from core MD95-2014) displays also an anomalously high Al/Ca content of 7337 mmol/mol compared to the other samples for which Al/Ca values are bellow 100 mmol/mol. For this sample, contamination by clay minerals is likely. Our observations suggest that the Fe-Mn oxide coatings, clay contamination (except for one sample) and/or foraminiferal test dissolution do not explain the too high Mg/Ca values of *G. bulloides* and the higher range of variability when compared with Δ_{47} values.

2) pH effect on the $\delta^{18}O$ measurements: $\delta^{18}O$-derived temperatures are used to correct the Mg/Ca; but the $\delta^{18}O$ of *G. bulloides* may be affected by pH effect (Spero et al., 1997; Spero et al., 1999; Zeebe, 1999). As a result, the high corrected Mg/Ca may be due to not considering the pH effect on $\delta^{18}O$. However, if the Mg/Ca is corrected using the temperature from the WOA rather than by the $\delta^{18}O$-derived temperature, the conclusion is similar: high corrected Mg/Ca is obtained. The pH effect on *G. bulloides* $\delta^{18}O$ cannot explain the high Mg/Ca ratio.

3) *G. bulloides* has been shown to present different morphotypes and also different genotypes (sometime with a similar morphotype), these cryptic species can potentially live at different depths and have specific ecological niches (Osborne et al., 2020). The Δ_{47} values of *G. bulloides* are in very good agreement with the other species used and do not show systematic biases (Fig. 3), suggesting that the singularity of *G. bulloides* data in the Mg/Ca. vs. Δ_{47} only occur in Mg/Ca ratio. The Δ_{47} SD of the *G. bulloides* measurements are good, suggesting that in any given sample, *G. bulloides* with the same morphotype and/or genotype were picked. However, we cannot exclude the possibility that different genotypes (with similar morphotype) were analyzed at different sites. More detailed studies on *G. bulloides* are

essential to better understand the potential cryptic variability of this species and its impact on Mg/Ca incorporation.

In the rest of the article, *G. bulloides* samples are removed from the dataset to better compare the corrected Mg/Ca and the clumped isotope-derived temperatures.

4.4. Salinity and pH effects on reconstructed Mg/Ca vs Δ_{47} temperatures

Considering that the Δ_{47} is independent of salinity and pH, and by correcting the Mg/Ca temperatures for each of these parameters, the observations made on figure 2 may be explained. In figure 5, we redraw the Mg/Ca-temperature.vs.Δ_{47}-temperature comparison of Figure 2d (i.e. obtained using the mono-specific calibration equations) but without *G. bulloides*. The mono-species Mg/Ca calibrations are corrected for salinity and pH (section 2.3.3). Using this corrected-mono-species calibrations for Mg/Ca-derived temperature, the comparison with Δ_{47}-derived temperatures is better; the regression line is close to the 1:1 line and explains 86% of the co-variance between both thermometers (Fig. 5). Thus, our results concur with observations from the geological record (Leutert et al, 2020; Meinecke et al 2021), that improved agreement between Δ_{47}-derived and Mg/Ca-derived temperatures is observed when the influences of pH and salinity on Mg/Ca are accounted. This emphasizes the importance of correcting Mg/Ca values for non-thermal influences. However, it is noticeable that cold Mg/Ca-derived temperatures still show a slight difference with Δ_{47}-derived temperatures. This could result from the small number of samples available and/or specific problems (e.g., effects of species, CO_3^{2-}). More data is requested on the cold end member to better understand this potential difference.

The good agreement between the Δ_{47}-derived temperatures and corrected Mg/Ca-derived temperatures provides further support that Δ_{47} is not affected by salinity (Tripati et al., 2010; Peral et al., 2018) and pH (or that the effect of pH is negligible).

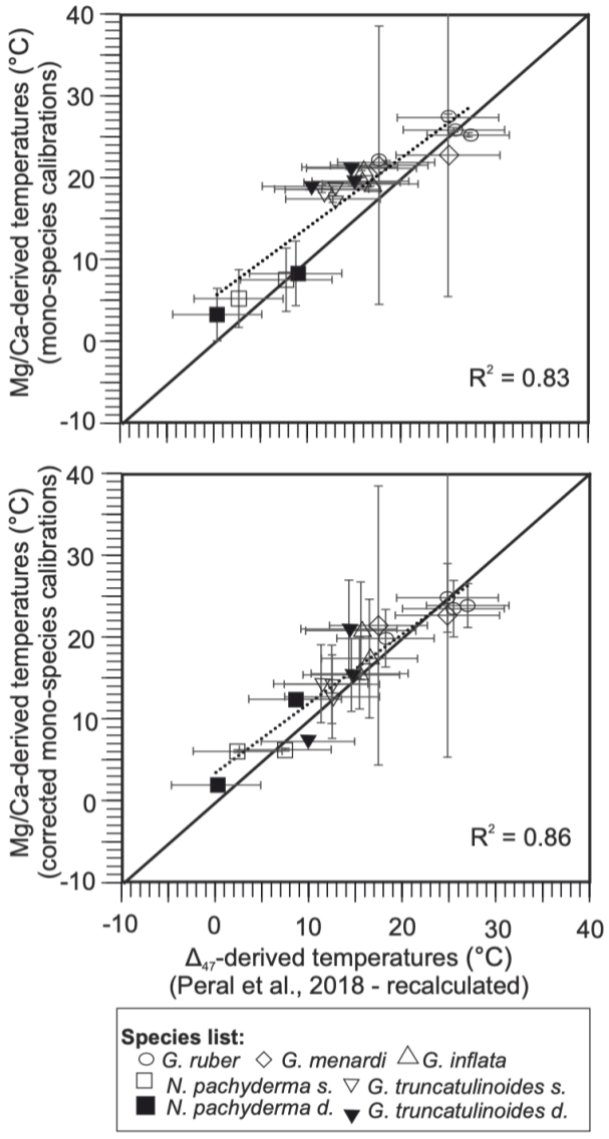

639

640 **Figure 5:** Mg/Ca-derived temperatures using mono-species calibrations, compared to the Δ_{47}-
641 derived temperatures using the recalculated Peral et al. (2018) calibration (a) and the Mg/Ca-
642 derived temperatures using the corrected Mg/Ca mono-species calibrations for salinity and
643 pH compared to the Δ_{47}-derived temperatures using the recalculated Peral et al. (2018)
644 calibration (b). The dotted linear regression, excluding *O. universa* and *G. bulloides*, is plotted.
645 A line 1:1 is plotted in black; uncertainties are at 2 SE.

646

647 **4.5. The potential of combining Mg/Ca ratio, $\delta^{18}O$ and Δ_{47} for palaeoceanographic studies**

648

649 The combination of $\delta^{18}O$ and Δ_{47} in foraminifera has been previously studied to
650 accurately reconstruct the signal of $\delta^{18}O_{sw}$ even during glacial-interglacial scales (Rodriguez-
651 Sanz et al., 2021; Peral et al., 2020). Next, the comparison between Mg/Ca and Δ_{47}

systematically shows differences between the two thermometers in modern and fossil foraminifera. Breitenbach et al. (2018) showed that combining Mg/Ca and clumped isotopes data may help to detect possible dissolution and metal coating biases on the Mg/Ca-thermometer. When samples are not biased by contamination, dissolution or diagenesis, the combination of these two proxies has been used to estimate long-term variations in seawater Mg/Ca (Evans et al., 2018; Meinecke et al., 2021).

In the present study, we showed that salinity and pH lead to discrepancies between clumped isotope and Mg/Ca in planktonic foraminifera frequently used for paleoceanographic reconstructions (however, further work is needed for *O. universa* and *G. bulloides*). Because of the multi-parameter dependency of foraminiferal $\delta^{18}O$, Δ_{47} and Mg/Ca, the combination of these paleo-thermometers could provide us with more than just the estimates of past ocean temperatures. Theoretically, based on the Gray and Evans equation (2019), the pH could be reconstructed by (i) solving the Mg/Ca dependency to temperature using Δ_{47}-derived temperatures and (ii) correcting for salinity using either the salinity estimated from sea level variations (Gray et al., 2019) or the salinity estimated from the combination of a thermometer (Δ_{47}-temperature or TEX_{86} as in Leutert et al. (2020)) and $\delta^{18}O$ (to obtain the $\delta^{18}O_{sw}$).

We tested such an approach with our core-top dataset. Firstly, $\delta^{18}O_{sw}$ was reconstructed by pairing $\delta^{18}O$ and Δ_{47} and using the equation 1 (Kim and O'Neil, 1997). Then salinity was reconstructed using modern salinity-$\delta^{18}O_{sw}$ relationships (section 2.4; supplementary material Fig. S4, at our site locations). Finally, we used our raw Mg/Ca, the estimated salinities and the clumped isotope temperatures to reconstruct pH values from the equations of Gray and Evans (2019). The reconstructed pH is compared to the pH extracted from the GLODAP 2020 data set (Olsen et al., 2020), by plotting their differences against the different species (Fig. 6). For each species, the differences between estimated- and atlas-pH (ΔpH) present a relatively good agreement, within the error bars, especially for *G. ruber* (Fig. 6). Part of the differences can be explained by the inaccurate assumptions regarding the depth of life and the optimal developmental season of foraminifera species, thus leading to incorrect pH being extracted from the atlases. Additionally, another limitation of this approach is the salinity reconstruction that we applied. It requires to assume that, in the past, the regional relationships between $\delta^{18}O_{sw}$ and salinity were the same as today. It is likely that in past climates, regional changes of evaporation/precipitation and isotopic fractionation during

683 atmospheric transport of water vapor, lead to changes in the $\delta^{18}O_{sw}$ – salinity relationship. On
684 a global scale, these changes may have also altered the impact of ice sheet waxing/waning on
685 the seawater $\delta^{18}O_{sw}$-salinity relationship. The extent and amount of sea ice may have also
686 decoupled this $\delta^{18}O_{sw}$- salinity relationship (LeGrande and Schmidt, 2011). A direct application
687 of the $\delta^{18}O$ and Δ_{47} combination is therefore not straightforward and other methods of salinity
688 reconstruction should be used (Gray and Evans, 2019; Leutert et al., 2020).

689 Thus, despite the theoretical potential of the approach described above, it should be
690 noted that the uncertainties in pH are large (at 2SE in Fig. 6), making the application of this
691 approach challenging. It is important to note that these uncertainties are particularly large
692 with respect to expected pH changes in the geological past (see discussion below). The
693 uncertainties in the reconstructed pH range between 0.23 and 0.39, which is too high for
694 useful paleoceanographic reconstruction and conversion to atmospheric CO_2 concentration,
695 since it has been estimated that pH variations over G-IG cycles are on the order of 0.15 (e.g.
696 Hönisch and Hemming, 2005; Henehan et al., 2013), and by 0.2 units over the Miocene
697 (Leutert et al., 2020)). In terms of propagation of errors, the estimated pH uncertainties are
698 dominated by the uncertainties in the clumped isotope-derived temperatures. The Δ_{47}
699 uncertainties need to be reduced by measuring more replicates or by improvements in mass
700 spectrometry.

701 Further studies and technical improvements are needed to improve species-specific
702 equations and better understand the dependence of Mg/Ca on salinity and pH, and to reduce
703 the amount of material needed for Δ_{47} measurements and decrease temperature
704 uncertainties. It is also mandatory to improve our knowledge about past relationships
705 between $\delta^{18}O_{sw}$ and salinity. While we are not able yet to fully benefit from the combination
706 of Mg/Ca, $\delta^{18}O$ and Δ_{47} ratios, the systematic use of these proxies is nonetheless useful to
707 better understand these proxies, their biases and thus help their interpretations in
708 paleoceanographic studies. Pairing these paleothermometers with the boron isotope pH
709 proxy (e.g., Foster and Rae, 2016), which requires knowledge of temperature to calculate K_B
710 and pH, would allow for multiple independent constraints on past variations in pH and
711 temperature.
712

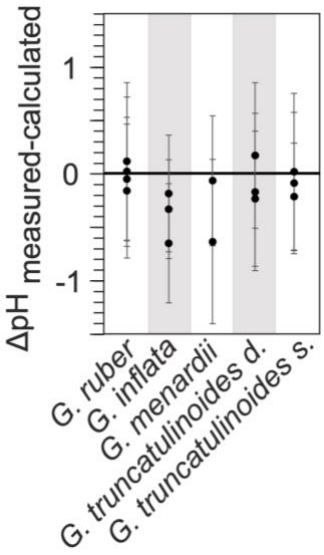

Figure 6: the difference for all the species from our dataset (excluding *O. universa, G. bulloides* and *N. pachyderma*) between the extracted pH from the atlas (GLOPAD 2020) and the reconstructed pH, using the equations from Gray and Evans (2019) with the raw Mg/Ca, the Δ_{47}-derived temperatures, and the combination of $\delta^{18}O$ and Δ_{47}-derived temperatures to reconstruct the $\delta^{18}Osw$. The uncertainties correspond to the uncertainties associated with the reconstructed pH (2SE)

5. CONCLUSION

The Mg/Ca in 7 planktonic foraminifer species is affected by species, salinity and pH effects (Gray et al., 2018). A strong correlation exists between Δ_{47} and Mg/Ca data when the later are corrected for salinity and pH effects with the Δ_{47} values. The *G. bulloides*-Mg/Ca ratio appear to show anomalously high values compared to the Mg/Ca-Δ_{47} relationship observed for the other seven planktonic species. Another process(es) may affect Mg/Ca in this species and additional investigation is needed to better understand what controls high Mg/Ca we observe in this species.

The improved agreement observed between Mg/Ca- and Δ_{47}-derived temperatures when Mg/Ca values are corrected for salinity and pH suggests that the foraminiferal clumped isotopes may only be temperature dependent. As such, the combination of the foraminiferal Mg/Ca, $\delta^{18}O$ and $\Delta_{47,}$ could allow the temperature (Δ_{47} thermometer), salinity (by combining $\delta^{18}O$ and Δ_{47}, to reconstruct the $\delta^{18}Osw$ and then, the salinity) and pH (the only remaining unknown) of the past seawater to be determined. However, at present, the application of this

later approach is nontrivial. In particular, the Δ_{47}-temperature uncertainties result in pH uncertainties higher than the expected pH changes in the geological record. Furthermore, the estimation of past salinity is also not straightforward. Finally, the species-specific Mg/Ca-pH sensitivity (Gray and Evans, 2019) adds an additional complication when applying the approach to extinct species.

This paper is also present an update of the foraminiferal clumped-isotope calibration of Peral et al. (2018), that benefits from the latest methodological developments (data processing and standardization) and can be directly applied to palaeoceanographic studies.

References

Anand P., Elderfield H. and Conte M. H. (2003) Calibration of Mg/Ca thermometry in planktonic foraminifera from a sediment trap time series. *Paleoceanography,* 18(2).

Anderson, N. T., Kelson, J. R., Kele, S., Daëron, M., Bonifacie, M., Horita, J., T. J. Mackey, C. M. John, T. Kluge, P. Petschnig, A. B. Jost, K. W. Huntinton, S. M. Bernasconi, Bergmann, K. D. (2021). A unified clumped isotope thermometer calibration (0.5–1100° C) using carbonate-based standardization. *Geophysical Research Letters*, e2020GL092069.

Barker S., Greaves M. and Elderfield H. (2003) A study of cleaning procedures used for foraminiferal Mg/Ca paleothermometry. Geochemistry, Geophys. Geosystems 4, 1–20.

Bemis, B. E., Spero, H. J., Bijma, J., & Lea, D. W. (1998). Reevaluation of the oxygen isotopic composition of planktonic foraminifera: Experimental results and revised paleotemperature equations. *Paleoceanography*, *13*(2), 150-160.

Bernasconi, S. M., Daëron, M., Bergmann, K. D., Bonifacie, M., Meckler, A. N., Affek, H. P., (n.d.). InterCarb: A community effort to improve inter-laboratory standardization of the carbonate clumped isotope thermometer using carbonate standards. *Geochemistry, Geophysics and Geosystems*. https://doi.org/10.1002/essoar.10504430.410.1002/essoar.10504430.3ems

Bernasconi S. M., Müller I. A., Bergmann K. D., Breitenbach S. F. M., Fernandez A., Hodell D. A., Jaggi M., Meckler A. N., Millan I. and Ziegler M. (2018) Reducing uncertainties in carbonate clumped isotope analysis through consistent 3 carbon- ate-based standardization. Geochem. Geophys, Geosyst.

Boyle, E. and Keigwin, L. (1985). Comparison of Atlantic and Pacific Paleochemical Records for the Last 215,000 Years - Changes in Deep Ocean Circulation and Chemical Inventories. Earth and Planetary Science Letters, 76:135–150.

Brand W. A., Assonov S. S. and Coplen T. B. (2010) Correction for the 17O interference in δ(13C) measurements when analyzing CO2 with stable isotope mass spectrometry (IUPAC Technical Report). Pure Appl. Chem. 82, 1719–1733. Available at: https://www.degruyter.com/view/j/pac.2010.82.issue-8/pac-rep-09-01-05/pac- rep-09-01-05.xml.

Breitenbach S. F. M., Mleneck-Vautravers M. J., Grauel A.-L., Lo L., Bernasconi S. M., Müller I. A., Rolfe J., Greaves M. and Hodell D. A. (2018) Coupled Mg/Ca and clumped isotope

analyses of foraminifera provide consis- tent water tempera- tures. Geochim. Cosmochim. Acta 236, 283–296.
Daëron, M., Blamart, D., Peral, M., & Affek, H. P. (2016). Absolute isotopic abundance ratios and the accuracy of Δ47 measurements. *Chemical Geology*, *442*, 83-96.
Daëron, M., Drysdale, R. N., Peral, M., Huyghe, D., Blamart, D., Coplen, T. B., ... & Zanchetta, G. (2019). Most Earth-surface calcites precipitate out of isotopic equilibrium. *Nature communications*, *10*(1), 1-7.
Daëron, M. (2021). Full propagation of analytical uncertainties in Δ47 measurements. *Geochemistry, Geophysics, Geosystems*, *22*(5), e2020GC009592.
de Villiers S., Greaves M. and Elderfield H. (2002) An intensity ratio calibration method for the accurate determination of Mg/Ca and Sr/Ca of marine carbonates by ICP- AES. Geochemistry, Geophys. Geosystems 3, n/a-n/a. Available at: http://doi.wiley.com/10.1029/2001GC000169.
Deuser, W. G., and E. H. Ross. 1989. Seasonally abundant planktonic foraminifera of the Saragossa Sea: Succession, deep-water fluxes, isotopic compositions, and paleoceanographic implications, J. Foraminiferal Res., 19, 268-293
Eiler, J.M. (2007) “Clumped-isotope” geochemistry-the study of naturally-occurring, multiply-substituted isotopologues. Earth Planet. Sci. Lett. 262, 309–327.
Eiler, J.M. (2011) Paleoclimate reconstruction using carbonate clumped isotope thermometry. Quat. Sci. Rev. 30 (25–26), 3575–3588. https://doi.org/10.1016/j. quascirev.2011.09.001
Elderfield H., Gansen G. (2000). Past temperature and $\boldsymbol{\delta}^{18}$O of surface ocean waters inferred from foraminiferal Mg/Ca ratios**.** *Nature*, 405, pp. 422-445
Elderfield, H., Vautravers, M., & Cooper, M. (2002). The relationship between shell size and Mg/Ca, Sr/Ca, δ18O, and δ13C of species of planktonic foraminifera. *Geochemistry, Geophysics, Geosystems*, *3*(8), 1-13.
Elderfield H., Yu J., Anand P., Kiefer T. and Nyland B. (2006) Calibrations for benthic foraminiferal Mg/Ca paleothermometry and the carbonate ion hypothesis. Earth Planet. Sci. Lett. 250, 633–649.
Elderfield H., Greaves M., Barker S., Hall I. R., Tripati A., Ferretti P., Crowhurst S., Booth L. and Daunt C. (2010) A record of bottom water temperature and seawater d 18 O for the Southern Ocean over the past 440 kyr based on Mg / Ca of benthic foraminiferal Uvigerina spp. Quat. Sci. Rev. 29, 160–169. Available at: http://dx.doi.org/10.1016/j.quascirev.2009.07.013.
Evans, D., Brierley, C., Raymo, M. E., Erez, J., & Müller, W. (2016). Planktic foraminifera shell chemistry response to seawater chemistry: Pliocene–Pleistocene seawater Mg/Ca, temperature and sea level change. *Earth and Planetary Science Letters*, *438*, 139-148.
Evans, D., Sagoo, N., Renema, W., Cotton, L. J., Müller, W., Todd, J. A., ... & Affek, H. P. (2018). Eocene greenhouse climate revealed by coupled clumped isotope-Mg/Ca thermometry. *Proceedings of the National Academy of Sciences*, *115*(6), 1174-1179.
Erez, J. (2003). The source of ions for biomineralization in foraminifera and their implications for paleoceanographic proxies. *Reviews in mineralogy and geochemistry*, *54*(1), 115-149.
Fiebig, J., Daëron, M., Bernecker, M., Guo, W., Schneider, G., Boch, R., Bernasconi, S., Jautzy, J., & Dietzel, M. (2021). Calibration of the dual clumped isotope thermometer for carbonates. *Geochimica et Cosmochimica Acta*, *312*, 235-256.

824 Foster, G. L., & Rae, J. W. (2016). Reconstructing ocean pH with boron isotopes in
825 foraminifera. *Annual Review of Earth and Planetary Sciences*, *44*, 207-237.
826 Grauel A. L., Schmid T. W., Hu B., Bergami C., Capotondi L., Zhou L. and Bernasconi S. M. (2013)
827 Calibration and application of the "clumped isotope" thermometer to foraminifera for
828 high-resolution climate reconstructions. Geochim. Cosmochim. Acta 108, 125–140.
829 Available at: http://dx.doi.org/10.1016/j.gca.2012.12.049.
830 Gray, W. R., Weldeab, S., Lea, D. W., Rosenthal, Y., Gruber, N., Donner, B., & Fischer, G. (2018).
831 The effects of temperature, salinity, and the carbonate system on Mg/Ca in
832 Globigerinoides ruber (white): A global sediment trap calibration. Earth and Planetary
833 Science Letters, 482, 607–620. https://doi.org/10.1016/j.epsl.2017.11.026
834 Gray, W. R., & Evans, D. (2019). Nonthermal influences on Mg/Ca in planktonic foraminifera:
835 A review of culture studies and application to the last glacial
836 maximum. *Paleoceanography and Paleoclimatology*, *34*(3), 306-315.
837 Hönisch, B., & Hemming, N. G. (2005). Surface ocean pH response to variations in pCO2
838 through two full glacial cycles. *Earth and Planetary Science Letters*, *236*(1-2), 305-314.
839 Henehan, M. J., Rae, J. W., Foster, G. L., Erez, J., Prentice, K. C., Kucera, M., ... & Elliott, T.
840 (2013). Calibration of the boron isotope proxy in the planktonic foraminifera
841 Globigerinoides ruber for use in palaeo-CO2 reconstruction. *Earth and Planetary Science*
842 *Letters*, *364*, 111-122.
843 Kim S.-T. and O'Neil J. R. (1997) Equilibrium and nonequilibrium oxygen isotope effects in
844 synthetic carbonates. Geochim. Cosmochim. Acta 61, 3461–3475. Available at:
845 http://linkinghub.elsevier.com/retrieve/pii/S0016703797001695.
846 Kisakürek, B., A. Eisenhauer, F. Böhm, D. Garbe-Schönberg, and J. Erez (2008), Controls on
847 shell Mg/Ca and Sr/Ca in cultured planktonic foraminiferan, Globigerinoides ruber
848 (white), Earth Planet. Sci. Lett., 273, 260–269, doi:10.1016/ j.epsl.2008.06.026.
849 Kissel C., Laj C., Mulder T., Wandres C. and Cremer M. (2009) The magnetic fraction: A tracer
850 of deep water circulation in the North Atlantic. Earth Planet. Sci. Lett. 288, 444–454.
851 https:// doi.org/10.1016/j.epsl.2009.10.005.
852 Kissel C., Van Toer A., Laj C., Cortijo E. and Michel E. (2013) Variations in the strength of the
853 North Atlantic bottom water during Holocene. Earth Planet. Sci. Lett. 369, 248–259.
854 Lea, D., T. Mashiotta, and H. Spero (1999), Controls on magnesium and strontium uptake in
855 planktonic foraminifera determined by live culturing, Geochim. Cosmochim. Acta, 63,
856 2369–2379, doi:10.1016/S0016-7037(99)00197-0.
857 Lea DW (2014) Elemental and isotopic proxies of past ocean temperatures. Treatise on
858 Geochemistry, eds Holland HD, Turekian KK (Elsevier, Amsterdam), 2nd Ed, pp 373–397.
859 Lear, C. H., Rosenthal, Y., & Slowey, N. (2002). Benthic foraminiferal Mg/Ca-
860 paleothermometry: A revised core-top calibration. *Geochimica et Cosmochimica*
861 *Acta*, *66*(19), 3375-3387.
862 LeGrande A. N. and Schmidt G. A. (2006) Global gridded data set of the oxygen isotopic
863 composition in seawater. Geophys. Res. Lett. 33, 1–5.
864 LeGrande, A. N., and Schmidt G. A. (2011), Water isotopologues as a quantitative paleosalinity
865 proxy, Paleoceanography, 26, PA3225, doi:10.1029/2010PA002043
866 Leutert, T. J., Auderset, A., Martínez-García, A., Modestou, S., & Meckler, A. N. (2020). Coupled
867 Southern Ocean cooling and Antarctic ice sheet expansion during the middle
868 Miocene. *Nature Geoscience*, *13*(9), 634-639.

Marchitto, T. M., Bryan, S. P., Curry, W. B., & McCorkle, D. C. (2007). Mg/Ca temperature calibration for the benthic foraminifer Cibicidoides pachyderma. *Paleoceanography*, *22*(1).

Marchitto T. M., Curry W. B., Lynch-Stieglitz J., Bryan S. P., Cobb K. M. and Lund D. C. (2014) Improved oxygen isotope temperature calibrations for cosmopolitan benthic foraminifera. Geochim. Cosmochim. Acta 130, 1–11. https://doi.org/ 10.1016/j.gca.2013.12.034.

Mathien-Blard E. and Bassinot F. (2009) Salinity bias on the foraminifera Mg/Ca thermometry: Correction procedure and implications for past ocean hydrographic reconstructions. Geochemistry, Geophys. Geosystems 10.

Meckler A. N., Ziegler M., Millán M. I., Breitenbach S. F. M. and Bernasconi S. M. (2014) Long-term performance of the Kiel carbonate device with a new correction scheme for clumped isotope measurements. Rapid Commun. Mass Spectrom. 28, 1705–1715.

Meinicke, N., Ho, S. L., Hannisdal, B., Nürnberg, D., Tripati, A., Schiebel, R., & Meckler, A. N. (2020). A robust calibration of the clumped isotopes to temperature relationship for foraminifers. *Geochimica et Cosmochimica Acta*, *270*, 160-183.

Meinicke, N., Reimi, M. A., Ravelo, A. C., & Meckler, A. N. Coupled Mg/Ca and clumped isotope measurements indicate lack of substantial mixed layer cooling in the Western Pacific Warm Pool during the last~ 5 million years. *Paleoceanography and Paleoclimatology*, e2020PA004115.

Mulitza, S., Boltovskoy, D., Donner, B., Meggers, H., Paul, A., Wefer, G. (2003) Temperature: δ18O relationships of planktonic foraminifera collected from surface waters. *Palaeogeography, Palaeoclimatology, Palaeoecology,* 202(1–2), 143-152. https://doi.org/10.1016/S0031-0182(03)00633-3.

Numberger, L., Hemleben, C., Hoffmann, R., Mackensen, A., Schulz, H., Wunderlich, J. M., & Kucera, M. (2009). Habitats, abundance patterns and isotopic signals of morphotypes of the planktonic foraminifer Globigerinoides ruber (d'Orbigny) in the eastern Mediterranean Sea since the Marine Isotopic Stage 12. Marine Micropaleontology, 73(1-2), 90-104.

Nürnberg, D., J. Bijma, and C. Hemleben (1996), Assessing the reliability of magnesium in foraminiferal calcite as a proxy for water mass temperatures, Geochim. Cosmochim. Acta, 60, 803–814, doi:10.1016/0016-7037(95)00446-7.

Olsen, A., Lange, N., Key, R M., Tanhua, T., Bittig, H C., Kozyr, A., Álvarez, M., Azetsu-Scott, K., Becker, S., Brown, P J., Carter, B R., da Cunha, L., Feely, R A., van Heuven, S., Hoppema, M., Ishii, M., Jeansson, E., Jutterström, S., Landa, C S., Lauvset, S K., Michaelis, P., Murata, A., Pérez, F F., Pfeil, B., Schirnick, C., Steinfeldt, R., Suzuki, T., Tilbrook, B., Velo, A., Wanninkhof, R., Woosley, R. J. (2020). An updated version of the global interior ocean biogeochemical data product, GLODAPv2. 2020. *Earth System Science Data*, *12*(4), 3653-3678.

Pang, X., Bassinot, F., & Sepulcre, S. (2020). Cleaning method impact on the Mg/Ca of three planktonic foraminifer species: A downcore study along a depth transect. *Chemical Geology*, *549*, 119690.

Oomori, T., Kaneshima, H., Maezato, Y., Kitano, Y., 1987. Distribution coefficient of Mg2+ ions between calcite and solution at 10–50°C. Marine Chemistry 20, pp. 327-336.

Osborne, E. B., Umling, N. E., Bizimis, M., Buckley, W., Sadekov, A., Tappa, E., ... & Thunell, R. C. (2020). A sediment trap evaluation of B/Ca as a carbonate system proxy in asymbiotic and nondinoflagellate hosting planktonic foraminifera. *Paleoceanography and Paleoclimatology*, *35*(2), e2019PA003682.

916 Passey, B. H., & Henkes, G. A. (2012). Carbonate clumped isotope bond reordering and
917 geospeedometry. *Earth and Planetary Science Letters*, *351*, 223-236.
918 Peral M., Daëron M., Blamart D., Bassinot F., Dewilde F., Smialkowski N., Isguder G., Jorissen
919 F., Kissel C., Michel E., Vázquez Riveiros, N. and Waelbroeck C. (2018) ScienceDirect
920 Updated calibration of the clumped isotope thermometer in planktonic and benthic
921 foraminifera. 239, 1–16.
922 Peral, M., Blamart, D., Bassinot, F., Daëron, M., Dewilde, F., Rebaubier, H., Nomade, S., Girone,
923 A., Marimo, M., Maiorano, P., & Ciaranfi, N. (2020). Changes in temperature and oxygen
924 isotopic composition of Mediterranean water during the Mid-Pleistocene transition in
925 the Montalbano Jonico section (southern Italy) using the clumped-isotope
926 thermometer. *Palaeogeography, Palaeoclimatology, Palaeoecology*, *544*, 109603.
927 Petersen, S. V., Defliese, W.F., Saenger, C., Daëron, M., John, C. M., Huntington, K. W., Kelson,
928 J. R., Bernasconi, S. M., Colman, A. S., Kluge, T., Olack, G. A., Schauer, A. J., Bajnai, D.,
929 Bonifacie, M., Breitenbach, S. F. M., Fiebig, J., Fernandez, A. B., Henkes, G. A., Hodell, D.,
930 Katz, A., Kele, S., Lohmann, K. C., Passey, B. H., Peral, M., Petrizzo, D. A., Rosenheim, B.
931 E., Tripati, A., Venturelli, R., Young, E. D., Wacker U., Winkelstern, I. Z. 2019. *Effects of*
932 *Improved ^{17}O Correction on Inter-Laboratory Agreement in Clumped Isotope*
933 *Calibrations, Estimates of Mineral-Specific Offsets, and Acid Fractionation Factor*
934 *Temperature Dependence.* Special Issue of Geochemistry, Geophysics, Geosystems, 20,
935 3495 – 3519
936 Piasecki, A., Bernasconi, S. M., Grauel, A., Hannisdal, B., Ho, S. L., Leutert, T. J., et al.
937 (2019). Application of clumped isotope thermometry to benthic
938 foraminifera. *Geochemistry, Geophysics, Geosystems*,
939 2018GC007961. https://doi.org/10.1029/2018GC007961
940 Regenberg, M., Steph, S., Nürnberg, D., Tiedemann, R., & Garbe-Schönberg, D. (2009).
941 Calibrating Mg/Ca ratios of multiple planktonic foraminiferal species with δ18O-
942 calcification temperatures: Paleothermometry for the upper water column. *Earth and*
943 *Planetary Science Letters*, *278*(3-4), 324-336.
944 Rebotim, A., Voelker, A. H., Jonkers, L., Waniek, J. J., Meggers, H., Schiebel, R., ... & Kucera, M.
945 (2017). Factors controlling the depth habitat of planktonic foraminifera in the
946 subtropical eastern North Atlantic. *Biogeosciences*, *14*(4), 827-859.
947 Retailleau, S., Schiebel, R., & Howa, H. (2011). Population dynamics of living planktic
948 foraminifers in the hemipelagic southeastern Bay of Biscay. *Marine*
949 *Micropaleontology*, *80*(3-4), 89-100.
950 Roche, D.M., C. Waelbroeck, B. Metcalfe, T. Caley, 2018. FAME (v1. 0): a simple module to
951 simulate the effect of planktonic foraminifer species-specific habitat on their oxygen
952 isotopic content. Geoscientific Model Development 11(9), 3587-3603.
953 Rodríguez-Sanz, L., Bernasconi, S.M., Marino, G. *et al.* Author Correction: Penultimate
954 deglacial warming across the Mediterranean Sea revealed by clumped isotopes in
955 foraminifera. *Sci Rep* **11**, 17511 (2021). https://doi.org/10.1038/s41598-021-96895-3
956 Rosenthal, Y., Boyle, E. A., & Slowey, N. (1997). Temperature control on the incorporation of
957 magnesium, strontium, fluorine, and cadmium into benthic foraminiferal shells from
958 Little Bahama Bank: Prospects for thermocline paleoceanography. *Geochimica et*
959 *Cosmochimica Acta*, *61*(17), 3633-3643.
960 Schauble E. A., Ghosh P. and Eiler J. M. (2006) Preferential formation of 13C-18O bonds in
961 carbonate minerals, estimated using first-principles lattice dynamics. Geochim.
962 Cosmochim. Acta 70, 2510–2529.

963 Shackleton N. (1967) Oxygen isotope analyses and Pleistocene temperatures re-assessed.
964 Nature 215, 15–17.
965 Shackleton N.J. (1974) Attainment of isotopic equilibrium between ocean water and
966 benthonic foraminifera genus *Uvigerina*: isotopic changes in the ocean during the last
967 glacial. Les méthodes quantitatives d'étude des variations du climat au cours du
968 Pleistocène, Gif-sur-Yvette. Colloque international du CNRS, 219, pp. 203-210
969 Spero H.J., Bijma J., Lea D.W., Bermis B.E. (1997) Effect of seawater carbonate concentration
970 on foraminiferal carbon and oxygen isotopes. *Nature*, 390, 497-500.
971 Spero H.J., Bijma J., Lea D.W., Russell, A.D. (1999) Deconvolving glacial ocean carbonate
972 chemistry from the planktonic foraminifera carbon isotope record.
973 F. Abrantes, A.C. Mix (Eds.), Reconstructing Ocean History: A Window into the
974 Future, Kluwer Academic/Plenum Publishers, New York, 329-342
975 Steinke, S., Chiu, H. Y., Yu, P. S., Shen, C. C., Löwemark, L., Mii, H. S., & Chen, M. T. (2005).
976 Mg/Ca ratios of two Globigerinoides ruber (white) morphotypes: Implications for
977 reconstructing past tropical/subtropical surface water conditions. Geochemistry,
978 Geophysics, Geosystems, 6(11).
979 Stewart, J. A., Christopher, S. J., Kucklick, J. R., Bordier, L., Chalk, T. B., Dapoigny, A., Douville,
980 E., Foster, G. L., Gray, W. R., Greenop, R., Gutjahr, M., Hemsing, F., Henehan, M. J.,
981 Holdship, P., Hsieh, Y., Kolevica, A., Lin, Y., Mawbey, E. M., Rae, J. W. B., Robinson, L. F.,
982 Shuttleworth, R., You, C., Zhang, S., & Day, R. D. (2021). NIST RM 8301 boron isotopes in
983 marine carbonate (simulated coral and foraminifera solutions): inter-laboratory δ11B
984 and trace element ratio value assignment. *Geostandards and Geoanalytical*
985 *Research*, *45*(1), 77-96.
986 Stolper D. A. and Eiler J. M. (2016) Constraints on the formation and diagenesis of
987 phosphorites using carbonate clumped isotopes. Geochim. Cosmochim. Acta 181, 238–
988 259.
989 Tierney, J. E., Malevich, S. B., Gray, W., Vetter, L., & Thirumalai, K. (2019). Bayesian calibration
990 of the Mg/Ca paleothermometer in planktic foraminifera. Paleoceanography and
991 Paleoclimatology, 34, 2005–2030. https://do.i org/10.1029/2019PA003744
992 Tripati A. K., Eagle R. A., Thiagarajan N., Gagnon A. C., Bauch H., Halloran P. R. and Eiler J. M.
993 (2010) 13C-18O isotope signatures and "clumped isotope" thermometry in foraminifera
994 and coccoliths. *Geochim. Cosmochim. Acta* 74, 5697–5717. Available at:
995 http://dx.doi.org/10.1016/j.gca.2010.07.006.
996 Tripati, A. K., Hill, P. S., Eagle, R. A., Mosenfelder, J. L., Tang, J., Schauble, E. A., ... & Henry, D.
997 (2015). Beyond temperature: Clumped isotope signatures in dissolved inorganic carbon
998 species and the influence of solution chemistry on carbonate mineral
999 composition. *Geochimica et Cosmochimica Acta*, *166*, 344-371.
1000 Urey, H.C., Lowenstam, H.A., Epstein, S. and McKinney, C.R. (1951): Measurements of
1001 paleotemperatures and temperatures of the Upper Cretaceous of England, Denmark
1002 and the southeastern United States. Bull. Geo. Soc. of Am., 62: 399-416.
1003 Vázquez Riveiros N., Govin A., Waelbroeck C., Mackensen A., Michel E., Moreira S., Bouinot T.,
1004 Caillon N., Orgun A. and Brandon M. (2016) Mg/Ca thermometry in planktic foramini-
1005 fera: improving paleotemperature estimations for G. bulloides and N. pachyderma left.
1006 Geochem. Geophy. Geosy. 17, 1249– 1264. https://doi.org/10.1002/2015GC006234
1007 Watkins, J. M., & Hunt, J. D. (2015). A process-based model for non-equilibrium clumped
1008 isotope effects in carbonates. *Earth and Planetary Science Letters*, *432*, 152-165.

Whitaker J., Khrulev C., Huard D., Paulik C., Hoyer S., Mohr F. A., Marquardt C., Couwenberg B., Bohnet M., Brett M., Hetland R., Korenčiak M., Onu K., Helmus J. J., Hamman J., Barna A., Koziol B., Kluyver T., May R., Smrekar J., Barker C., Davar G., Cournapeau D., da Silva D., Gohlke C., Kinoshita B. P. (2019). Unidata/netcdf4-pythin: version 1.4.3.2 release (v1.4.3.2). Zenodo. https://doi.org/10.5281/zenodo.2592291

Yu, J.M., Day, J., Greaves, M., Elderfield, H., 2005. Determination of multiple element/calcium ratios in foraminiferal calcite by quadrupole ICP-MS. Geochem. Geophys. Geosyst. 6, Q08P01. doi:10.1029/2005GC000964.

Zeebe R.E. (1999). An explanation of the effect of seawater carbonate concentration on foraminiferal oxygen isotopes. Geochim. Cosmochim. Acta, 63, 2001-2007.

Zweng, M.M, J.R. Reagan, J.I. Antonov, R.A. Locarnini, A.V. Mishonov, T.P. Boyer, H.E. Garcia, O.K. Baranova, D.R. Johnson, D.Seidov, M.M. Biddle, 2013. *World Ocean Atlas 2013, Volume 2: Salinity.* S. Levitus, Ed., A. Mishonov Technical Ed.; NOAA Atlas NESDIS 74, 39 pp.

Author contributions

MP and FB have designed the study. MP wrote the manuscript, and all co-authors help in the writing. MD provided the python code to reprocess the clumped-isotope calibration. FB, DB, MD and WG provided assistance in the interpretation of the clumped-isotope and/or Mg/Ca data. JB, FJ, CK, EM and CW helped in the selection of the marine sediment cores and foraminifer species. MP hand-picked the foraminiferal samples. MP and HR cleaned the samples for the Mg/Ca measurements and HR and WG performed the Mg/Ca measurements.

Acknowledgements

All authors thank the editor for his patience in the lengthy process of reviewing this article and the 3 anonymous reviewers for their really useful comments that significantly improve the manuscript. MP thanks the CEA for the financially support during her 3-years PhD fellowship 2015-2018.

Table 1: Core top locations and water depth with species considered in this study and chronological.

Cores	Latitude (°)	Longitude (°)	Water depth (m)	Species	Core-top cal. yrs BP (95% CL)	References
MOCOSEDst1	73.04	-11.93	1839	*Cibicides wuellerstorfi; N. pachyderma s*	6317 (+150/-94) *	(1)
MD04-2720	-49.13	71.36	750	*N. pachyderma d*	n.a.	
MD12-3401	-44.69	80.4	3445	*G. bulloides*	< 4000 **	(2)
MD95-2014	60.59	-22.08	2397	*G. bulloides*	715 (+94/-149) *	(1)
MD08-3182Q	52.71	-35.94	1355	*N. pachyderma s; G. bulloides*	500 (+40/–53) *	(3)
MD03-2680Q	61.06	-24.55	1812	*N. pachyderma d*	402	(4)
2FPA1	43.67	-2.00	664	*Uvigerina mediterranea*	< 4000 ***	(1)
SU90I-03	40.05	-30	2475	*G. bulloides*	2013 (+125/-120) *	(1)
MD08-3179Q	37.86	-30.3	2036	*G. ruber; G. inflata; G. truncatulinoides s; G. truncatulinoides d*	4403 (+153/-121) *	(1)
MD12-3426Q	19.73	114.61	3630	*G. menardii; O. universa*	1755 (+159/-139) *	(1)
MD00-2360	-20.08	112.67	980	*G. menardii; O. universa; G. ruber*	3622 (+135/-137) *	(1)
MD02-2577Q	28.84	-86.67	4076	*G. menardii; O. universa; G. ruber*	1107 (+110/-105) *	(1)

* Age determined by radiocarbon dating
** Age determined by stratigraphic control
*** Age determined by presence of Rose Bengal
(1) Peral et al., 2018; (2) Vazquez Riveiros et al., 2016; (3) Kissel et al., 2013 and (4) Kissel et al., 2009

Table 2: Summary of the main results used in this study. The samples/species are represented with the optimal size fraction. The raw Mg/Ca values are presented, as well as the $\delta^{18}Oc$ and the recalculated Δ_{47} values with their associated uncertainties at 1SE. We also present the corrected Mg/Ca values for salinity and pH. Seawater salinity from WOA and pH from GLODAP 2020 (Olsen et al., 2020), are reported.

Core	Species	Optimal Size	δ18Oc	SE	Δ47	SE	Mg/Ca	SE	Mg/Ca	SE	pH	SE
			VPDB (‰)		(‰)		raw		corrected		reconstructed	
MD08-3182	*G. bulloides*	250-315	1.77	0.1	0.6489	0.0074	2.10	0.006	2.24	0.309	7.941	0.27
MD08-3182	*G. bulloides*	315-355	1.87	0.1	0.665	0.0074	2.06	0.006	2.20	0.300	7.571	0.28
MD12-3401	*G. bulloides*	250-315	2.04	0.1	0.6626	0.0075	1.45	0.006	1.64	0.144	8.041	0.23
MD95-2014	*G. bulloides*	315-355	2.13	0.1	0.6492	0.0074	4.69	0.006	4.86	0.211	7.044	0.39
SU90-03	*G. bulloides*	250-315	1.59	0.1	0.6429	0.0063	3.30	0.006	3.44	0.427	7.570	0.30
MD08-3179	*G. inflata*	355-400	1.19	0.1	0.6286	0.0074	2.03	0.008	2.10	0.328	8.283	0.31
MD08-3179	*G. inflata*	400-450	1.08	0.1	0.6219	0.0073	1.68	0.008	1.76	0.339	8.747	0.29
MD08-3179	*G. inflata*	450-500	1.24	0.1	0.6247	0.0085	2.00	0.008	2.08	0.323	8.429	0.35
MD00-2360	*G. menardi menardi*	355-400	-0.37	0.1	0.5977	0.0075	2.85	0.004	3.15	0.354	8.741	0.37
MD00-2360	*G. menardi menardi*	400-450	-0.29	0.1	0.619	0.0074	2.55	0.004	2.84	0.346	8.170	0.34
MD00-2360	*G. ruber*	250-315	-1.76	0.1	0.5917	0.0058	4.34	0.008	4.88	0.643	8.262	0.32
MD02-2577	*G. ruber*	250-315	-1.33	0.1	0.5959	0.0073	4.59	0.008	4.71	0.813	8.099	0.37
MD02-2577	*G. ruber*	315-355	-1.46	0.1	0.5977	0.0073	4.63	0.008	4.75	0.847	8.029	0.37
MD08-3179	*G. ruber*	250-315	-0.08	0.1	0.6167	0.0073	3.21	0.008	3.37	0.597	7.988	0.33
MD08-3179	*G. truncatulinoides (d.)*	355-400	1.05	0.1	0.6424	0.0074	1.97	0.006	2.05	0.345	7.926	0.25
MD08-3179	*G. truncatulinoides (d.)*	400-450	1.14	0.1	0.6251	0.0074	2.09	0.006	2.16	0.336	8.331	0.34
MD08-3179	*G. truncatulinoides (d.)*	450-500	1.07	0.1	0.6278	0.0074	2.06	0.006	2.14	0.342	8.268	0.33
MD08-3179	*G. truncatulinoides (s.)*	355-400	1.08	0.1	0.638	0.0074	1.91	0.006	1.99	0.341	8.080	0.28
MD08-3179	*G. truncatulinoides (s.)*	400-450	1.07	0.1	0.6343	0.0074	1.90	0.006	1.98	0.342	8.184	0.30
MD08-3179	*G. truncatulinoides (s.)*	450-500	1.17	0.1	0.6342	0.0074	1.72	0.006	1.79	0.332	8.312	0.31
MD03-2680	*N. pachyderma (d.)*	200-250	1.73	0.1	0.647	0.0074	1.16	0.008	1.184	0.008		
MD04-2720	*N. pachyderma (d.)*	200-250	3.24	0.1	0.676	0.0075	0.76	0.008	0.87	0.008		
MD08-3182	*N. pachyderma (s.)*	200-250	1.76	0.1	0.6504	0.0074	1.09	0.006	1.17	0.006		
MOCOSED	*N. pachyderma (s.)*	200-250	2.86	0.1	0.6678	0.0074	0.90	0.006	1.15	0.006		

Table 3: Summary of all the Mg/Ca calibration used in this study: mono-specific species calibrations, calibration with salinity and pH corrections and the salinity and pH corrected multi-species calibration

Recalculated multi-species calibration from Anand et al., 2003					
Mg/Ca = B*exp(A*T)					
		Values	SE		
	A	0.0913	0.003		Recalculated in this study
	B	0.6109	0.002		
Mono-specific calibrations					
Mg/Ca = B*exp(A*T)					
		Values	SE	Size fraction	
G. menardii	A	0.091	0.012	355-400	Regenberg et al., 2009
	B	0.36	0.31		
O. universa	A	0.085	0.002	NA	Lea et al., 1999
	B	1.38	0.05		
G. ruber	A	0.09		350-500	Anand et al., 2003
	B	0.595	0.042		
	A	0.09		250-350	
	B	0.449	0.006		
	A	0.09		350-500	
	B	0.395	0.009		
N. pachyderma s	A	0.084	0.006	200-250	Vasquez Riveiros et al., 2016
	B	0.58	0.084		
G. inflata	A	0.09		350-500	Anand et al., 2003
	B	0.299	0.005		
G. truncatulinoides d.	A	0.09		350-500	
	B	0.359	0.008		
G. truncatulinoides s.	A	0.09		350-500	
	B	0.359	0.008		
G. bulloides	A	0.081	0.005	250-315	Elderfield and Ganssen. 2000 North Atlantic
	B	0.81	0.04		
	A	0.061	0.005	250-315	Elderfield and Ganssen. 2000 Southern Ocean
	B	0.996	0.038		
Mono-specific calibrations with SSS and pH corrections					
Mg/Ca=exp(A*(S - B) + C*T + D*(pH - E) + F					
		Values	SE		
G. ruber	A	0.036	0.006		Gray and Evans. 2019
	B	35			
	C	0.061	0.005		
	D	-0.87	0.1		
	E	8	0		
	F	0.03	0.03		
G. bulloides	A	0.036	0.006		
	B	35			
	C	0.061	0.005		
	D	-0.88	0.12		
	E	8	0		
	F	0.21	0.04		
O. universa	A	0.036	0.006		
	B	35			
	C	0.061	0.005		
	D	-0.51	0.11		
	E	8	0		
	F	0.77	0.48		
Multi-species	A	0.036	0.006		
	B	35			
	C	0.061	0.005		
	D	-0.73	0.07		
	E	8	0		
	F	0			

Step 1

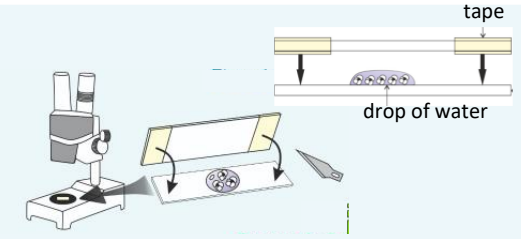

Step 2

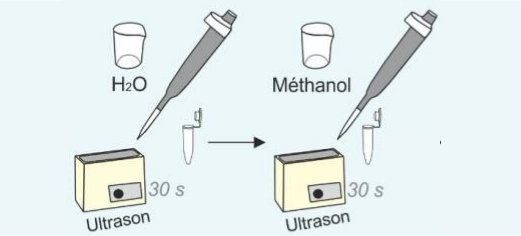

Step 3

Cleaning protocol for clumped isotope in foraminifera

Step 1: Crush the foraminifera

Gently crush foraminifera between two glass slides to open all chambers

Step 2: remove clay

Add milliQ water
Remove the water
Ultrasonic bath for 30s
Repeat 3 times or more until water remains clear and colourless

Add methanol
Ultrasonic bath for 30s
Remove the methanol
Repeat 2 time or more until the methanol remains clear and colourless

Remove the maximum of the methanol

Step 3: Dry

Dry at room temperature under a fume hood. Microtubes should be open but covered with aluminum foil to avoid dust contaminants

Equipment:
Microtubes, gloves, fume hood, microscope, 4 beaker (for water & dirty water and for methanol & dirty methanol), pipette and pipette tip (change for each sample or each step)

Figure S1: summary of the cleaning protocol steps for clumped isotope in foraminifera

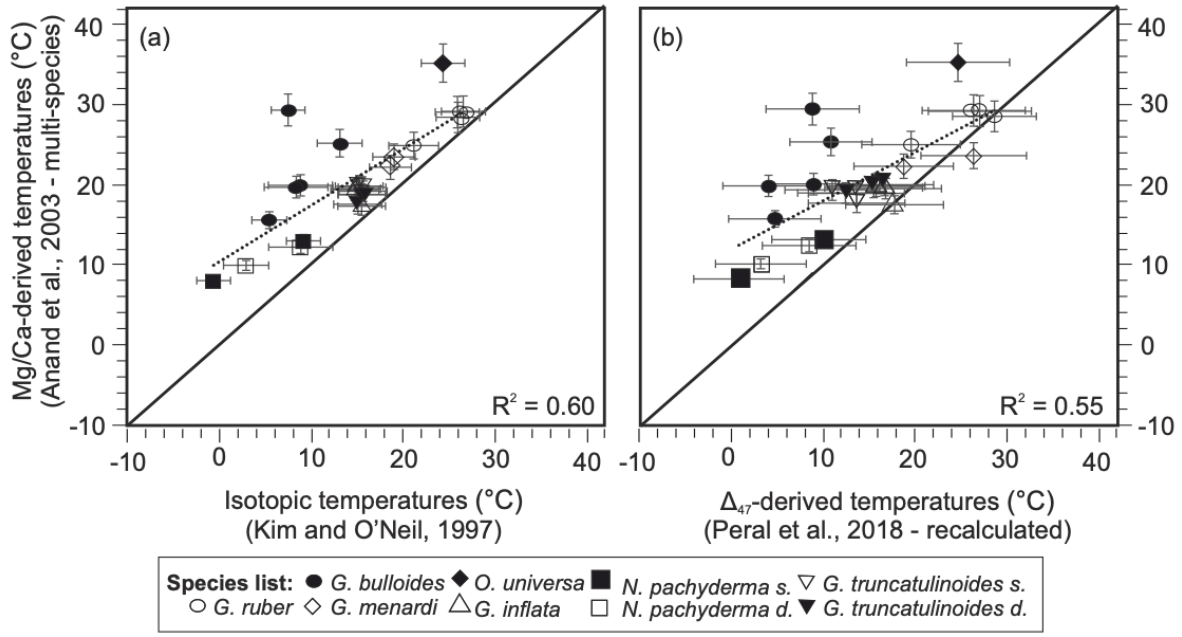

Figure S2: reconstructed Mg/Ca temperatures using the original multi-species calibration of Anand et al. (2003) compared to reconstructed $\delta^{18}O$ temperatures, using Kim and O'Neil (1997) (a) and Δ_{47}-derived temperatures, using recalculated Peral et al. (2018) (b) for 9 planktic foraminifera. The linear regressions are the dotted black lines, a line 1:1 is in black, and the uncertainties are at 2 SE. The Mg/Ca-derived temperatures are systematically higher than the isotopic-derived temperatures.

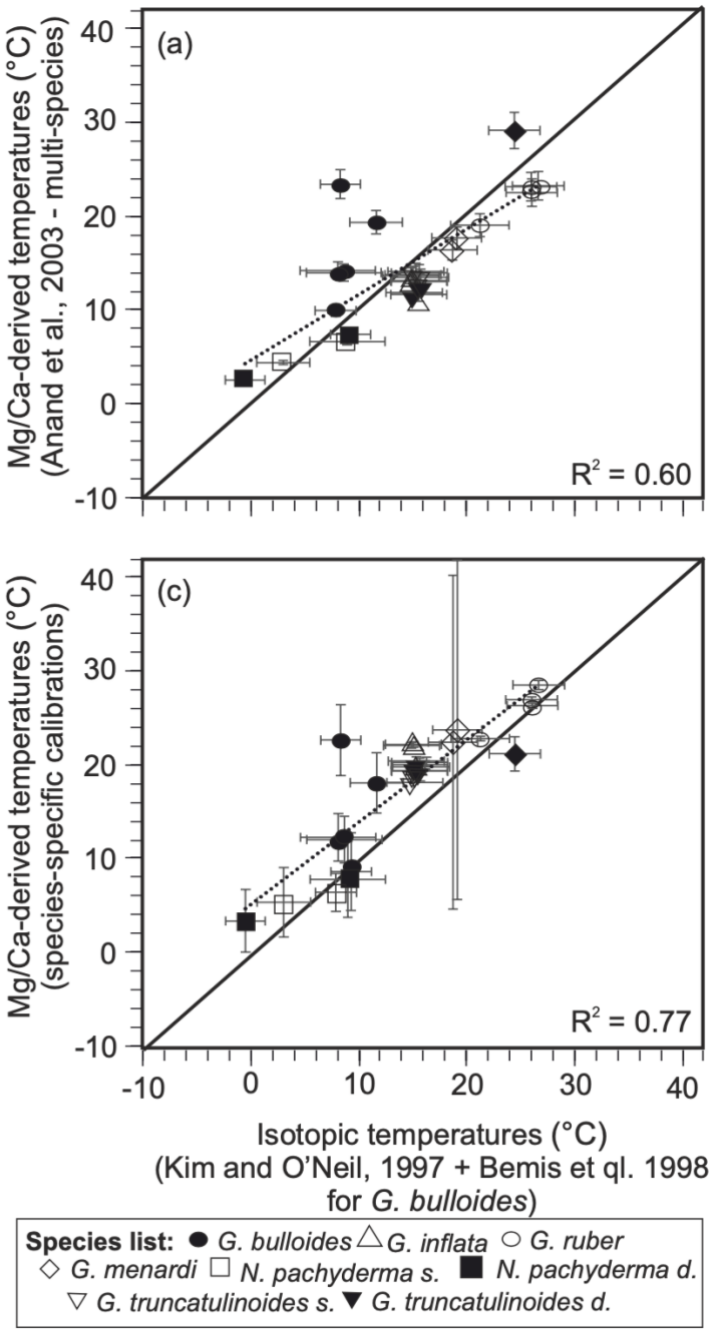

Figure S3: reconstructed Mg/Ca temperatures using the recalculated multi-species calibration of Anand et al. (2003) compared to reconstructed $\delta^{18}O$ temperatures, using Kim and O'Neil (1997) (a) and reconstructed Mg/Ca derived temperatures using the most adequate mono-specific calibrations compared to reconstructed $\delta^{18}O$ temperatures, using Kim and O'Neil (1997) and Bemis et al. (1998) calibration for *G. bulloides* (b). The linear regressions are the dotted black lines, the 1:1 line is the black solid line, and the uncertainties are at 2 SE.

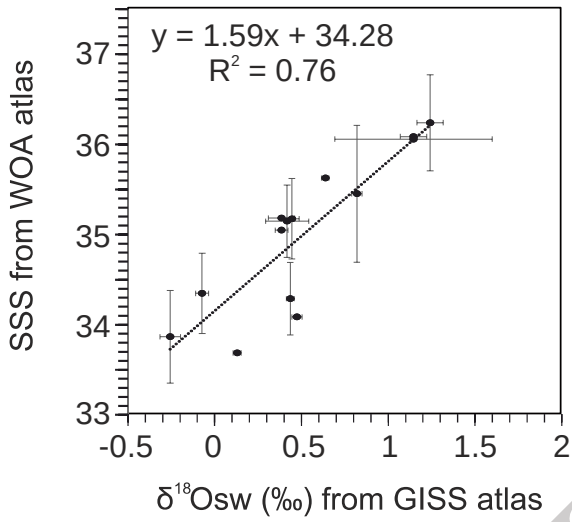

Figure S4: relationship between the seawater salinity from WOA 13 and the $\delta^{18}O$ of the seawater from GISS atlas for all our samples defined as core/species. For benthic foraminifera we used the available bottom data and planktonic foraminifera we integrated data withing the column water corresponding to the known living depths of each specie (see details in Peral et al., 2018). The linear regressions are the dotted black lines, a line 1:1 is in black, and the uncertainties are at 2 SE.

Figure 1: Map of core-top location used in this study, with the mean annual SST from WOA13

Figure 2: Comparison of temperature estimates obtained on 9 planktonic species. Top panels: reconstructed Mg/Ca temperatures using the recalculated multi-species calibration of Anand et al. (2003) compared to reconstructed $\delta^{18}O$ temperatures, using Kim and O'Neil (1997) (a) and Δ_{47}-derived temperatures, using recalculated Peral et al. (2018) (b). Bottom panel: reconstructed Mg/Ca derived temperatures using the most adequate mono-specific calibrations compared to reconstructed $\delta^{18}O$ temperatures, using Kim and O'Neil (1997) (c) and Δ_{47}-derived temperatures, using recalculated Peral et al. (2018) calibration (d). Dotted black lines are linear regressions, the black solid lines are the 1:1 line. Uncertainties are at 2SE.

Figure 3: Comparison of our recalculated foraminiferal Δ_{47} values with raw Mg/Ca values (uncorrected) (a), with corrected Mg/Ca for salinity only (b), and with corrected Mg/Ca for salinity and pH (c). The Mg/Ca values are corrected using the equations from Gray and Evans (2019), the salinity and pH from the atlas and the oxygen isotopic temperatures. The red dotted logarithmic regressions are plotted for all the plots, including *G. bulloides* and the black regressions are without *G. bulloides*. All the uncertainties are at 2SE.

Figure 4: Recalculated Δ_{47} values (mean and 2SE) compared to oxygen isotopic temperatures (mean and 2SE) obtained with Kim and O'Neil (1997) for planktonic (circle) and benthic (square) foraminifera samples, combining all size fractions (modified from Peral et al., 2018). The new calibration regression corresponds to the black line (Peral et al., 2018 recalculated). The recalculated foraminiferal calibration is compared to the slow-growing calcite from Laghetto Basso and Devils Hole (from Anderson et al., 2021) and to calibrations of Anderson et al. (2021) and Fiebig et al. (2021)

Figure 5: Mg/Ca-derived temperatures using mono-species calibrations, compared to the Δ_{47}-derived temperatures using the recalculated Peral et al. (2018) calibration (a) and the Mg/Ca-derived temperatures using the corrected Mg/Ca mono-species calibrations for salinity and pH compared to the Δ_{47}-derived temperatures using the recalculated Peral et al. (2018) calibration (b). The dotted linear regression, excluding *O. universa* and *G. bulloides*, is plotted. A line 1:1 is plotted in black; uncertainties are at 2 SE.

Figure 6: the difference for all the species from our dataset (excluding *O. universa, G. bulloides* and *N. pachyderma*) between the extracted pH from the atlas (GLOPAD 2020) and the reconstructed pH, using the equations from Gray and Evans (2019) with the raw Mg/Ca, the Δ_{47}-derived temperatures, and the combination of $\delta^{18}O$ and Δ_{47}-derived temperatures to reconstruct the $\delta^{18}Osw$. The uncertainties correspond to the uncertainties associated with the reconstructed pH (2SE)